

**Supersymmetric  $SO(10)$ -inspired GUTs with sliding scales**Carolina Arbeláez,<sup>\*</sup> Renato M. Fonseca,<sup>†</sup> and Jorge C. Romão<sup>‡</sup>*Departamento de Física and CFTP, Technical University of Lisbon, Avenida Rovisco Pais 1, 1049-001 Lisboa, Portugal*Martin Hirsch<sup>§</sup>*AHEP Group, Instituto de Física Corpuscular-C.S.I.C./Universitat de València Edificio de Institutos de Paterna, Apartado 22085, E-46071 València, Spain*

(Received 31 January 2013; published 12 April 2013)

We construct lists of supersymmetric models with extended gauge groups at intermediate steps, all of which are inspired by  $SO(10)$  unification. We consider three different kinds of setups: (i) the model has exactly one additional intermediate scale with a left-right (LR) symmetric group; (ii)  $SO(10)$  is broken to the LR group via an intermediate Pati-Salam scale; and (iii) the LR group is broken into  $SU(3)_c \times SU(2)_L \times U(1)_R \times U(1)_{B-L}$ , before breaking to the standard model (SM) group. We use sets of conditions, which we call the “sliding mechanism,” which yield unification with the extended gauge group(s) allowed at arbitrary intermediate energy scales. All models thus can have new gauge bosons within the reach of the LHC, in principle. We apply additional conditions, such as perturbative unification, renormalizability and anomaly cancellation and find that, despite these requirements, for the ansatz (i) with only one additional scale still around 50 different variants exist that can have a LR symmetry below 10 TeV. For the more complicated schemes (ii) and (iii) literally thousands of possible variants exist, and for scheme (ii) we have also found variants with very low Pati-Salam scales. We also discuss possible experimental tests of the models from measurements of supersymmetry masses. Assuming mSUGRA boundary conditions we calculate certain combinations of soft terms, called “invariants,” for the different classes of models. Values for all the invariants can be classified into a small number of sets, which contain information about the class of models and, in principle, the scale of beyond-minimal supersymmetric extension of the Standard Model physics, even in case the extended gauge group is broken at an energy beyond the reach of the LHC.

DOI: [10.1103/PhysRevD.87.075010](https://doi.org/10.1103/PhysRevD.87.075010)

PACS numbers: 14.60.Pq, 12.60.Jv

**I. INTRODUCTION**

In the minimal supersymmetric extension of the Standard Model (MSSM) gauge couplings unify at an energy scale of about  $m_G \simeq 2 \times 10^{16}$  GeV. Adding particles arbitrarily to the MSSM easily destroys this attractive feature. Thus, relatively few supersymmetry (SUSY) models have been discussed in the literature which have a larger than MSSM particle content at experimentally accessible energies. Neutrino oscillation experiments [1–3], however, have shown that at least one neutrino must have a mass  $m_{\text{Atm}} \geq 0.05$  eV.<sup>1</sup> A (Majorana) neutrino mass of this order indicates the existence of a new energy scale below  $m_G$ . For models with renormalizable interactions and perturbative couplings, as for example in the classical seesaw models [5–8], this new scale should lie below approximately  $\Lambda_{\text{LNV}} \lesssim 10^{15}$  GeV.

From the theoretical point of view grand unified theory (GUT) models based on the group  $SO(10)$  [9] offer a number of advantages compared to the simpler models based on  $SU(5)$ . For example, several of the chains

through which  $SO(10)$  can be broken to the SM gauge group contain the left-right (LR) symmetric group  $SU(3)_c \times SU(2)_L \times SU(2)_R \times U(1)_{B-L}$  as an intermediate step [10], thus potentially explaining the observed left-handedness of the weak interactions. However, probably the most interesting aspect of  $SO(10)$  is that it automatically contains the necessary ingredients to generate a seesaw mechanism [8]: (i) the right-handed neutrino is included in the **16**-plet which forms a fermion family; and (ii)  $(B - L)$  is one of the generators of  $SO(10)$ .

$SO(10)$  based models with an intermediate LR symmetry usually break the LR symmetry at a rather large energy scale,  $m_R$ . For example, Refs. [11,12] use **210** and a pair of **126** and  $\overline{\mathbf{126}}$  to break  $SO(10)$  and conclude that, under certain assumptions about the supersymmetry breaking scale,  $m_R$  has to be larger than roughly  $10^{10}$  GeV. Similar conclusions were reached in Ref. [13,14], where **45**, **54** and a pair of **126** and  $\overline{\mathbf{126}}$  were used to break  $SO(10)$ . Also in SUSY LR models inspired by these  $SO(10)$  constructions usually  $m_R$  is assumed to be quite large. For example, if LR is broken in the SUSY LR model by the vacuum expectation value (VEV) of  $(B - L) = 2$  triplets [15,16] or by a combination of  $(B - L) = 2$  and  $(B - L) = 0$  triplets [17,18],  $m_R \simeq 10^{15}$  GeV is the typical scale consistent with gauge coupling unification (GCU). The authors of Ref. [19] find a lower limit of

<sup>\*</sup>Carolina.Arbelaez@ist.utl.pt<sup>†</sup>renato.fonseca@ist.utl.pt<sup>‡</sup>jorge.romao@ist.utl.pt<sup>§</sup>mahirsch@ific.uv.es<sup>1</sup>For the latest fits of oscillation data, see for example Ref. [4].

$m_R \gtrsim 10^9$  GeV from GCU for models where the LR symmetry is broken by triplets, even if one allows additional nonrenormalizable operators or sizable GUT-scale thresholds to be present. On the other hand, in models with an extended gauge group it is possible to formulate sets of conditions on the  $\beta$  coefficients for the gauge couplings, which allow us to enforce GCU independent of the energy scale at which the extended gauge group is broken. This was called the “sliding mechanism” in Ref. [20].<sup>2</sup> However, [20] was not the first to present examples of “sliding scale” models in the literature. In Ref. [22] it was shown that, if the left-right group is broken to  $SU(2)_L \times U(1)_R \times U(1)_{B-L}$  by the vacuum expectation value of a scalar field  $\Phi_{1,1,3,0}$  then<sup>3</sup> the resulting  $U(1)_R \times U(1)_{B-L}$  can be broken to  $U(1)_Y$  of the SM in agreement with experimental data at any energy scale. In Ref. [19] the authors demonstrated that in fact a complete LR group can be lowered to the TeV scale, if certain carefully chosen fields are added and the LR symmetry is broken by right doublets. A particularly simple model of this kind was discussed in Ref. [23]. Finally, the authors of Ref. [20] discussed also an alternative way of constructing a sliding LR scale by relating it to an intermediate Pati-Salam stage. We note in passing that these papers are not in contradiction with the earlier work [15–18], which all have to have large  $m_R$ . As discussed briefly in the next section it is not possible to construct a sliding scale variant for a LR model including pairs of  $\Phi_{1,1,3,-2}$  and  $\Phi_{1,3,1,-2}$ .

Three different constructions, based on different  $SO(10)$  breaking chains, were considered in Ref. [20]. In chain I  $SO(10)$  is broken in exactly one intermediate (LR symmetric) step to the standard model group:

$$\begin{aligned} SO(10) &\rightarrow SU(3)_c \times SU(2)_L \times SU(2)_R \times U(1)_{B-L} \\ &\rightarrow \text{MSSM}. \end{aligned} \quad (1)$$

In chain II  $SO(10)$  is broken first to the Pati-Salam group [24]:

$$\begin{aligned} SO(10) &\rightarrow SU(4) \times SU(2)_L \times SU(2)_R \\ &\rightarrow SU(3)_c \times SU(2)_L \times SU(2)_R \times U(1)_{B-L} \\ &\rightarrow \text{MSSM}. \end{aligned} \quad (2)$$

And finally, in chain III,

$$\begin{aligned} SO(10) &\rightarrow SU(3)_c \times SU(2)_L \times SU(2)_R \times U(1)_{B-L} \\ &\rightarrow SU(3)_c \times SU(2)_L \times U(1)_R \times U(1)_{B-L} \\ &\rightarrow \text{MSSM}. \end{aligned} \quad (3)$$

In all cases the last symmetry breaking scale before reaching the SM group can be as low as  $\mathcal{O}(1)$  TeV maintaining

<sup>2</sup>A different (but related) approach to enforcing GCU is taken by the authors of Ref. [21] with what they call “magic fields.”

<sup>3</sup>The indices are the transformation properties under the LR group; see the next section and the Appendix for notation.

nevertheless GCU.<sup>4</sup> The papers discussed above [19,20,22,23] give at most one or two example models for each chain, i.e., they present a “proof of principle” that models with the stipulated conditions indeed can be constructed in agreement with experimental constraints. It is then perhaps natural to ask: How unique are the models discussed in these papers? The answer we find for this question is, perhaps unsurprisingly, that a huge number of variants exist in each class. Even in the simplest class (chain I) we have found a total of 53 variants (up to 5324 configurations; see next section) which can have perturbative GCU and a LR scale below 10 TeV, consistent with experimental data. For the two other classes, chain II and chain III, we have found literally thousands of variants.

With such a huge number of variants of essentially “equivalent” constructions one immediate concern is whether there is any way of distinguishing among all of these constructions experimentally. Tests could be either direct or indirect. Direct tests are possible, because of the sliding scale feature of the classes of models we discuss; see Sec. II. Different variants predict different additional (s)particles, some of which (being colored) could give rise to spectacular resonances at the LHC. However, even if the new gauge symmetry and all additional fields are outside the reach of the LHC, all variants have different  $\beta$  coefficients and thus different running of MSSM parameters, both gauge couplings and SUSY soft masses. Thus, if one assumes the validity of a certain SUSY breaking scheme, such as for example mSugra, indirect traces of the different variants remain in the SUSY spectrum, potentially measurable at the LHC and a future ILC/CLIC. This was discussed earlier in the context of indirect tests for the SUSY seesaw mechanism in Refs. [25–27] and for extended gauge models in Ref. [20]. We generalize the discussion of Ref. [20] and show how the “invariants,” i.e., certain combinations of soft SUSY breaking parameters, can themselves be organized into a few classes, which in principle allow us to distinguish class-II models from class I or class III and, if sufficient precision could be reached experimentally, even select specific variants within a class and give indirect information about the new energy scale(s).

The rest of this paper is organized as follows: in the next section we first lay out the general conditions for the construction of the models we are interested in, before discussing variants and example configurations for all of the three classes we consider. Section III then discusses invariants, i.e., SUSY soft parameters in the different model classes. We then close with a short summary and discussion. Several technical aspects of our work are presented in the Appendix.

<sup>4</sup>In fact, the sliding mechanism would work also at even lower energy scales. This possibility is, however, excluded phenomenologically.

## II. MODELS

### A. Supersymmetric $SO(10)$ models: General considerations

Before entering into the details of the different model classes, we will first list some general requirements which we use in all constructions. These requirements are the basic conditions any model has to fulfill to guarantee at least in principle that a phenomenologically realistic model will result.

We use the following conditions:

- (i) Perturbative  $SO(10)$  unification. That is, gauge couplings unify (at least) as well as in the MSSM and the value of  $\alpha_G$  is in the perturbative regime.
- (ii) The GUT scale should lie above (roughly)  $10^{16}$  GeV. This bound is motivated by the limit on the proton decay half-life.
- (iii) Sliding mechanism. This requirement is a set of conditions (different conditions for different classes of models) on the allowed  $\beta$  coefficients of the gauge couplings, which ensure the additional gauge group structure can be broken at any energy scale consistent with GCU.
- (iv) Renormalizable symmetry breaking. This implies that at each intermediate step we assume there are (at least) the minimal number of Higgs fields, which the corresponding symmetry breaking scheme requires.
- (v) Fermion masses and in particular neutrino masses. This condition implies that the field content of the extended gauge groups is rich enough to fit experimental data, although we will not attempt detailed fits of all data. In particular, we require the fields to generate Majorana neutrino masses through seesaw, either ordinary seesaw or inverse/linear seesaw, to be present.<sup>5</sup>
- (vi) Anomaly cancellation. We accept as valid models only field configurations which are anomaly free.
- (vii)  $SO(10)$  completable. All fields used in a lower energy stage must be parts of a multiplet present at the next higher symmetry stage. In particular, all fields should come from the decomposition of one of the  $SO(10)$  multiplets we consider (multiplets up to **126**).
- (viii) Correct MSSM limit. All models must be rich enough in particle content that at low energies the MSSM can emerge.

A few more words on our naming convention and notations might be necessary. We consider the three different  $SO(10)$  breaking chains, Eqs. (1)–(3), and will call these model “classes.” In each class there are fixed sets of  $\beta$  coefficients, which all lead to GCU but with different

values of  $\alpha_G$  and different values of  $\alpha_R$  and  $\alpha_{B-L}$  at low energies. These different sets are called “variants” in the following. And finally, (nearly) all of the variants can be created by more than one possible set of superfields. We will call such a set of superfields a “configuration.” Configurations are what usually is called “model” by model builders, although we prefer to think of these as “protomodels,” i.e., constructions fulfilling all our basic requirements. These are only protomodels (and not full-fledged models), since we do not check for each configuration in a detailed calculation that all the fields required in that configuration can remain light. We believe that for many, but probably not all, of the configurations one can find conditions for the required field combinations being “light,” following similar conditions as discussed in the prototype class-I model of Ref. [23].

All superfields are named as  $\Phi_{3_c, 2_L, 2_R, 1_{B-L}}$  (in the left-right symmetric stage),  $\Psi_{4, 2_L, 2_R}$  (in the Pati-Salam regime) and  $\Phi'_{3_c, 2_L, 1_R, 1_{B-L}}$  [in the  $U(1)_R \times U(1)_{B-L}$  regime], with the indices giving the transformation properties under the group. A conjugate of a field is denoted by, for example,  $\Phi_{3_c, 2_L, 2_R, 1_{B-L}}$ , however, without putting a corresponding “bar” (or minus sign) in the index. We list all fields we use, together with their transformation properties and their origin from  $SO(10)$  multiplets, complete up to the **126** of  $SO(10)$  in the Appendix.

### B. Model class I: One intermediate (left-right) scale

We start our discussion with the simplest class of models with only one new intermediate scale (LR):

$$SO(10) \rightarrow SU(3)_c \times SU(2)_L \times SU(2)_R \times U(1)_{B-L} \rightarrow \text{MSSM}. \quad (4)$$

We do not discuss the first symmetry breaking step in detail, since it is not relevant for the following discussion and only mention that  $SO(10)$  can be broken to the LR group either via the interplay of VEVs from a **45** and a **54**, as done for example in Ref. [23], or via a **45** and a **210**, an approach followed in Ref. [22]. In the left-right symmetric stage we consider all irreducible representations, which can be constructed from  $SO(10)$  multiplets up to dimension **126**. This allows for a total of 24 different representations (plus conjugates); their transformation properties under the LR group and their  $SO(10)$  origin are summarized in Table IV (and Table V) of the Appendix.

Consider gauge coupling unification first. If we take the MSSM particle content as a starting point, the  $\beta$  coefficients in the different regimes are given as<sup>6</sup>

<sup>5</sup>For  $SO(10)$  based models including fit to fermion masses (also neutrinos) see, for example, Refs. [28,29].

<sup>6</sup>For  $b_1^{\text{SM}}$  and  $b_2^{\text{SM}}$  we use the SM particle content plus one additional Higgs doublet.

$$\begin{aligned}
(b_3^{\text{SM}}, b_2^{\text{SM}}, b_1^{\text{SM}}) &= (-7, -3, 21/5) \\
(b_3^{\text{MSSM}}, b_2^{\text{MSSM}}, b_1^{\text{MSSM}}) &= (-3, 1, 33/5) \\
(b_3^{\text{LR}}, b_2^{\text{LR}}, b_R^{\text{LR}}, b_{B-L}^{\text{LR}}) &= (-3, 1, 1, 6) \\
&+ (\Delta b_3^{\text{LR}}, \Delta b_2^{\text{LR}}, \Delta b_R^{\text{LR}}, \Delta b_{B-L}^{\text{LR}}),
\end{aligned} \tag{5}$$

where we have used the canonical normalization for  $(B-L)$  related to the physical one by  $(B-L)^c = \sqrt{\frac{3}{8}}(B-L)^p$ . Here,  $\Delta b_i^{\text{LR}}$  stands for the contributions from additional superfields, not accounted for in the MSSM.

As is well known, while the MSSM unifies, putting an additional LR scale below the GUT scale with  $\forall \Delta b_i^{\text{LR}} = 0$  destroys unification. Nevertheless GCU can be maintained, if some simple conditions on the  $\Delta b_i^{\text{LR}}$  are fulfilled. First, since in the MSSM  $\alpha_3 = \alpha_2$  at roughly  $2 \times 10^{16}$  GeV one has that  $\Delta b_2^{\text{LR}} = \Delta b_3^{\text{LR}} \equiv \Delta b$  in order to preserve this situation for an arbitrary LR scale (sliding condition). Next, recall the matching condition

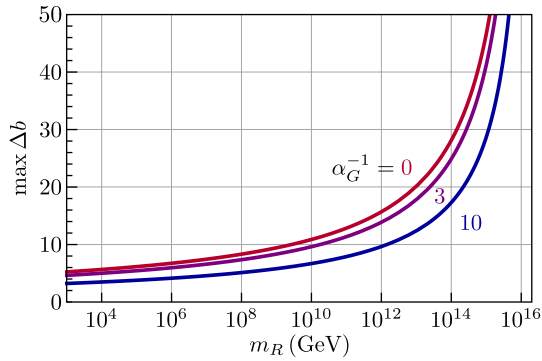
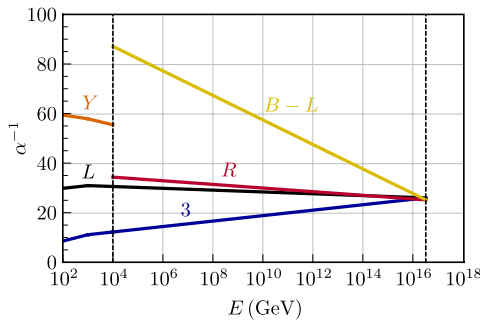


FIG. 1 (color online). Maximum value of  $\Delta b$  allowed by perturbativity as function of the scale  $m_R$  in GeV. The three different lines have been calculated for three different values for the unified coupling  $\alpha_G^{-1}$ , namely  $\alpha_G^{-1} = 0, 3, 10$ . A LR scale below 10 TeV (1 TeV) requires  $\text{Max}(\Delta b_3) \leq 5.7$  (5.2) if the extreme value of  $\alpha_G^{-1} = 0$  is chosen and  $\text{Max}(\Delta b_3) \leq 5.1$  (4.7) for  $\alpha_G^{-1} = 3$ .



$$\alpha_1^{-1}(m_R) = \frac{3}{5}\alpha_R^{-1}(m_R) + \frac{2}{5}\alpha_{B-L}^{-1}(m_R), \tag{6}$$

which, by substitution of the LR scale by an arbitrary one above  $m_R$ , allows us to define an artificial continuation of the hypercharge coupling constant  $\alpha_1$  into the LR stage. The  $\beta$  coefficient of this dummy coupling constant for  $E > m_R$  is  $\frac{3}{5}b_R^{\text{LR}} + \frac{2}{5}b_{B-L}^{\text{LR}}$  and it should be compared with  $b_1^{\text{MSSM}}$  ( $E < m_R$ ); the difference is  $\frac{3}{5}\Delta b_R^{\text{LR}} + \frac{2}{5}\Delta b_{B-L}^{\text{LR}} - \frac{18}{5}$  and it must be equal to  $\Delta b$  in order for the difference between this  $\alpha_1$  coupling and  $\alpha_3 = \alpha_2$  at the GUT to be independent of the scale  $m_R$ . These are the two conditions imposed by the sliding requirement of the LR scale on the  $\beta$  coefficients [see Eq. (7)]. Note, however, that we did not require (approximate) unification of  $\alpha_R$  and  $\alpha_{B-L}$  with  $\alpha_3$  and  $\alpha_2$ ; it was sufficient to require that  $\alpha_2^{-1} = \alpha_3^{-1} \approx \frac{3}{5}\alpha_R^{-1} + \frac{2}{5}\alpha_{B-L}^{-1}$ . In any case, we can always achieve the desired unification because the splitting between  $\alpha_R$  and  $\alpha_{B-L}$  at the  $m_R$  scale is a free parameter, so it can be used to force  $\alpha_R = \alpha_{B-L}$  at the scale where  $\alpha_3$  and  $\alpha_2$  unify, which leads to an almost perfect unification of the four couplings. Also, we require that unification is perturbative, i.e., the value of the common coupling constant at the GUT scale is  $\alpha_G^{-1} \geq 0$ . From the experimental value of  $\alpha_5(m_Z)$  [30] one can easily calculate the maximal allowed value of  $\Delta b$  as a function of the scale, where the LR group is broken to the SM group. This is shown in Fig. 1 for three different values of  $\alpha_G^{-1}$ . The smallest  $\text{Max}(\Delta b)$  is obtained for the smallest value of  $m_R$  (and the largest value of  $\alpha_G^{-1}$ ). For  $\alpha_G^{-1}$  in the interval  $[0, 3]$  one obtains  $\text{Max}(\Delta b)$  in the range  $[4.7, 5.7]$ , i.e., we will study cases up to a  $\text{Max}(\Delta b) = 5$  (see, however, the discussion below).

All together these considerations result in the following constraints on the allowed values for the  $\Delta b_i^{\text{LR}}$ :

$$\begin{aligned}
\Delta b_2^{\text{LR}} = \Delta b_3^{\text{LR}} = \Delta b &\leq 5, \\
\Delta b_{B-L}^{\text{LR}} + \frac{3}{2}\Delta b_R^{\text{LR}} - 9 &= \frac{5}{2}\Delta b \leq \frac{25}{2}.
\end{aligned} \tag{7}$$

Given Eq. (7) one can calculate all allowed variants of sets of  $\Delta b_i^{\text{LR}}$  guaranteed to give GCU. Two examples are shown in Fig. 2. The figure shows the running of the inverse gauge

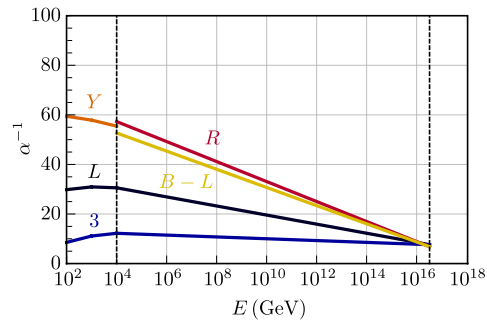


FIG. 2 (color online). Gauge coupling unification in LR models for  $m_R = 10^4$  GeV. The left panel is for  $(\Delta b_3^{\text{LR}}, \Delta b_2^{\text{LR}}, \Delta b_R^{\text{LR}}, \Delta b_{B-L}^{\text{LR}}) = (0, 0, 1, 15/2)$  and the right panel is for  $(4, 4, 10, 4)$ .

TABLE I. List of the 53 variants with a single LR scale. Shown are the 29 variants with  $\Delta b_3 < 4$ . In each case, the fields shown are the extra ones which are needed besides the ones contained in the MSSM representations (the two-Higgs doublets are assumed to come from one bidoublet  $\Phi_{1,2,2,0}$ ). The  $\Delta b_3$ ,  $\Delta b_2$ ,  $\Delta b_R$ ,  $\Delta b_{B-L}$  values can be obtained from the first column through Eqs. (7).

$(\Delta b, \Delta b_R)$	Sample field combination
(0, 1)	$\bar{\Phi}_{1,1,2,-1} + 2\bar{\Phi}_{1,1,1,2} + \Phi_{1,1,2,-1} + 2\Phi_{1,1,1,2}$
(0, 2)	$2\bar{\Phi}_{1,1,2,-1} + \bar{\Phi}_{1,1,1,2} + 2\Phi_{1,1,2,-1} + \Phi_{1,1,1,2}$
(0, 3)	$\bar{\Phi}_{1,1,2,-1} + \bar{\Phi}_{1,1,1,2} + \Phi_{1,1,2,-1} + \Phi_{1,1,3,0} + \Phi_{1,1,1,2}$
(0, 4)	$2\bar{\Phi}_{1,1,2,-1} + 2\Phi_{1,1,2,-1} + \Phi_{1,1,3,0}$
(0, 5)	$\bar{\Phi}_{1,1,2,-1} + \Phi_{1,1,2,-1} + 2\Phi_{1,1,3,0}$
(1, 1)	$\bar{\Phi}_{1,2,1,1} + \bar{\Phi}_{1,1,2,-1} + 2\bar{\Phi}_{1,1,1,2} + \bar{\Phi}_{3,1,1,-\frac{2}{3}} + \Phi_{1,2,1,1} + \Phi_{1,1,2,-1} + 2\Phi_{1,1,1,2} + \Phi_{3,1,1,-\frac{2}{3}}$
(1, 2)	$\bar{\Phi}_{1,1,2,-1} + 2\bar{\Phi}_{1,1,1,2} + \bar{\Phi}_{3,1,1,-\frac{2}{3}} + \Phi_{1,1,2,-1} + \Phi_{1,2,2,0} + 2\Phi_{1,1,1,2} + \Phi_{3,1,1,-\frac{2}{3}}$
(1, 3)	$2\bar{\Phi}_{1,1,2,-1} + \bar{\Phi}_{1,1,1,2} + \bar{\Phi}_{3,1,1,-\frac{2}{3}} + 2\Phi_{1,1,2,-1} + \Phi_{1,2,2,0} + \Phi_{1,1,1,2} + \Phi_{3,1,1,-\frac{2}{3}}$
(1, 4)	$\bar{\Phi}_{1,1,2,-1} + \bar{\Phi}_{1,1,1,2} + \bar{\Phi}_{3,1,1,-\frac{2}{3}} + \Phi_{1,1,2,-1} + \Phi_{1,1,3,0} + \Phi_{1,2,2,0} + \Phi_{1,1,1,2} + \Phi_{3,1,1,-\frac{2}{3}}$
(1, 5)	$2\bar{\Phi}_{1,1,2,-1} + \bar{\Phi}_{3,1,1,-\frac{2}{3}} + 2\Phi_{1,1,2,-1} + \Phi_{1,1,3,0} + \Phi_{1,2,2,0} + \Phi_{3,1,1,-\frac{2}{3}}$
(1, 6)	$\bar{\Phi}_{1,1,2,-1} + \bar{\Phi}_{3,1,1,-\frac{2}{3}} + \Phi_{1,1,2,-1} + 2\Phi_{1,1,3,0} + \Phi_{1,2,2,0} + \Phi_{3,1,1,-\frac{2}{3}}$
(2, 1)	$\bar{\Phi}_{1,1,2,-1} + 3\bar{\Phi}_{1,1,1,2} + 2\bar{\Phi}_{3,1,1,-\frac{2}{3}} + \Phi_{1,1,2,-1} + \Phi_{1,3,1,0} + 3\Phi_{1,1,1,2} + 2\Phi_{3,1,1,-\frac{2}{3}}$
(2, 2)	$2\bar{\Phi}_{1,1,2,-1} + 2\bar{\Phi}_{1,1,1,2} + 2\bar{\Phi}_{3,1,1,-\frac{2}{3}} + 2\Phi_{1,1,2,-1} + \Phi_{1,3,1,0} + 2\Phi_{1,1,1,2} + 2\Phi_{3,1,1,-\frac{2}{3}}$
(2, 3)	$\bar{\Phi}_{1,1,2,-1} + 2\bar{\Phi}_{1,1,1,2} + 2\bar{\Phi}_{3,1,1,-\frac{2}{3}} + \Phi_{1,1,2,-1} + 2\Phi_{1,2,2,0} + 2\Phi_{1,1,1,2} + 2\Phi_{3,1,1,-\frac{2}{3}}$
(2, 4)	$2\bar{\Phi}_{1,1,2,-1} + \bar{\Phi}_{1,1,1,2} + 2\bar{\Phi}_{3,1,1,-\frac{2}{3}} + 2\Phi_{1,1,2,-1} + 2\Phi_{1,2,2,0} + \Phi_{1,1,1,2} + 2\Phi_{3,1,1,-\frac{2}{3}}$
(2, 5)	$\bar{\Phi}_{1,1,2,-1} + \bar{\Phi}_{1,1,1,2} + 2\bar{\Phi}_{3,1,1,-\frac{2}{3}} + \Phi_{1,1,2,-1} + \Phi_{1,1,3,0} + 2\Phi_{1,2,2,0} + \Phi_{1,1,1,2} + 2\Phi_{3,1,1,-\frac{2}{3}}$
(2, 6)	$2\bar{\Phi}_{1,1,2,-1} + 2\bar{\Phi}_{3,1,1,-\frac{2}{3}} + 2\Phi_{1,1,2,-1} + \Phi_{1,1,3,0} + 2\Phi_{1,2,2,0} + 2\Phi_{3,1,1,-\frac{2}{3}}$
(2, 7)	$\bar{\Phi}_{1,1,2,-1} + 2\bar{\Phi}_{3,1,1,-\frac{2}{3}} + \Phi_{1,1,2,-1} + 2\Phi_{1,1,3,0} + 2\Phi_{1,2,2,0} + 2\Phi_{3,1,1,-\frac{2}{3}}$
(2, 8)	$\bar{\Phi}_{1,1,2,-1} + \bar{\Phi}_{3,1,2,\frac{1}{3}} + \Phi_{1,1,2,-1} + \Phi_{1,1,3,0} + 2\Phi_{1,2,2,0} + \Phi_{3,1,2,\frac{1}{3}}$
(3, 1)	$\bar{\Phi}_{1,2,1,1} + \bar{\Phi}_{1,1,2,-1} + 4\bar{\Phi}_{1,1,1,2} + \Phi_{1,2,1,1} + \Phi_{1,1,2,-1} + \Phi_{1,3,1,0} + \Phi_{8,1,1,0} + 4\Phi_{1,1,1,2}$
(3, 2)	$\bar{\Phi}_{1,1,2,-1} + 4\bar{\Phi}_{1,1,1,2} + \bar{\Phi}_{1,1,2,-1} + \Phi_{1,3,1,0} + \Phi_{1,2,2,0} + \Phi_{8,1,1,0} + 4\Phi_{1,1,1,2}$
(3, 3)	$2\bar{\Phi}_{1,1,2,-1} + 3\bar{\Phi}_{1,1,1,2} + 2\Phi_{1,1,2,-1} + \Phi_{1,3,1,0} + \Phi_{1,2,2,0} + \Phi_{8,1,1,0} + 3\Phi_{1,1,1,2}$
(3, 4)	$\bar{\Phi}_{1,2,1,1} + \bar{\Phi}_{1,1,3,-2} + \bar{\Phi}_{1,2,1,1} + \Phi_{1,3,1,0} + \Phi_{8,1,1,0} + \Phi_{1,1,3,-2}$
(3, 5)	$\bar{\Phi}_{1,1,3,-2} + \Phi_{1,3,1,0} + \Phi_{1,2,2,0} + \Phi_{8,1,1,0} + \Phi_{1,1,3,-2}$
(3, 6)	$\bar{\Phi}_{1,1,2,-1} + 2\bar{\Phi}_{1,1,1,2} + \Phi_{1,1,2,-1} + \Phi_{1,1,3,0} + 3\Phi_{1,2,2,0} + \Phi_{8,1,1,0} + 2\Phi_{1,1,1,2}$
(3, 7)	$2\bar{\Phi}_{1,1,2,-1} + \bar{\Phi}_{1,1,1,2} + 2\Phi_{1,1,2,-1} + \Phi_{1,1,3,0} + 3\Phi_{1,2,2,0} + \Phi_{8,1,1,0} + \Phi_{1,1,1,2}$
(3, 8)	$\bar{\Phi}_{1,1,2,-1} + \bar{\Phi}_{1,1,1,2} + \bar{\Phi}_{1,1,2,-1} + 2\Phi_{1,1,3,0} + 3\Phi_{1,2,2,0} + \Phi_{8,1,1,0} + \Phi_{1,1,1,2}$
(3, 9)	$2\bar{\Phi}_{1,1,2,-1} + 2\Phi_{1,1,2,-1} + 2\Phi_{1,1,3,0} + 3\Phi_{1,2,2,0} + \Phi_{8,1,1,0}$
(3, 10)	$\bar{\Phi}_{1,1,2,-1} + \bar{\Phi}_{1,1,2,-1} + 3\Phi_{1,1,3,0} + 3\Phi_{1,2,2,0} + \Phi_{8,1,1,0}$

couplings as a function of the energy scale, for an assumed value of  $m_R = 10$  TeV and a SUSY scale of 1 TeV, for  $(\Delta b_3^{\text{LR}}, \Delta b_2^{\text{LR}}, \Delta b_R^{\text{LR}}, \Delta b_{B-L}^{\text{LR}}) = (0, 0, 1, 15/2)$  (left) and  $(4, 4, 10, 4)$  (right). The example on the left has  $\alpha_G^{-1} \simeq 25$  as in the MSSM, while the example on the right has  $\alpha_G^{-1} \simeq 6$ . Note that while both examples lead by construction to the same value of  $\alpha_1(m_Z)$ , they have very different values for  $\alpha_R(m_R)$  and  $\alpha_{B-L}(m_R)$  and thus predict different couplings for the gauge bosons  $W_R$  and  $Z'$  of the extended gauge group.

With the constraints from Eq. (7), we find that a total of 65 different variants can be constructed. However, after imposing that at least one of the fields that breaks correctly

the  $SU(2)_R \times U(1)_{B-L}$  symmetry to  $U(1)_Y$  is present, either a  $\Phi_{1,1,3,-2}$  or a  $\Phi_{1,1,2,-1}$  (and/or their conjugates), the number of variants is reduced to 53. We list them in Tables I and II, together with one example of field configurations which give the corresponding  $\Delta b_i^{\text{LR}}$ .

We give only one example for each configuration in Tables I and II, although we went through the exercise of finding all possible configurations for the 53 variants with the field content of Table IV. In total there are 5324 anomaly-free configurations [31]. Only the variants (0, 1), (0, 2), (0, 4) and (0, 5) have only one configuration, while larger numbers of configurations are usually found for larger values of  $\Delta b_3^{\text{LR}}$ .

TABLE II. List of the 53 variants with a single LR scale. Shown are the remaining 24 variants, with  $\Delta b_3 \geq 4$ .

$(\Delta b, \Delta b_R)$	Sample field combination
(4, 1)	$\bar{\Phi}_{1,1,2,-1} + 5\bar{\Phi}_{1,1,1,2} + \bar{\Phi}_{3,1,1,-\frac{2}{3}} + \Phi_{1,1,2,-1} + 2\Phi_{1,3,1,0} + \Phi_{8,1,1,0} + 5\Phi_{1,1,1,2} + \Phi_{3,1,1,-\frac{2}{3}}$
(4, 2)	$2\bar{\Phi}_{1,1,2,-1} + 4\bar{\Phi}_{1,1,1,2} + \bar{\Phi}_{3,1,1,-\frac{2}{3}} + 2\Phi_{1,1,2,-1} + 2\Phi_{1,3,1,0} + \Phi_{8,1,1,0} + 4\Phi_{1,1,1,2} + \Phi_{3,1,1,-\frac{2}{3}}$
(4, 3)	$\bar{\Phi}_{1,1,2,-1} + 4\bar{\Phi}_{1,1,1,2} + \bar{\Phi}_{3,1,1,-\frac{2}{3}} + \Phi_{1,1,2,-1} + \Phi_{1,3,1,0} + 2\Phi_{1,2,2,0} + \Phi_{8,1,1,0} + 4\Phi_{1,1,1,2} + \Phi_{3,1,1,-\frac{2}{3}}$
(4, 4)	$\bar{\Phi}_{1,1,1,2} + \bar{\Phi}_{3,1,1,-\frac{2}{3}} + \bar{\Phi}_{1,1,3,-2} + 2\Phi_{1,3,1,0} + \Phi_{8,1,1,0} + \Phi_{1,1,1,2} + \Phi_{3,1,1,-\frac{2}{3}} + \Phi_{1,1,3,-2}$
(4, 5)	$\bar{\Phi}_{1,1,2,-1} + \bar{\Phi}_{3,1,1,-\frac{2}{3}} + \bar{\Phi}_{1,1,3,-2} + \Phi_{1,1,2,-1} + 2\Phi_{1,3,1,0} + \Phi_{8,1,1,0} + \Phi_{3,1,1,-\frac{2}{3}} + \Phi_{1,1,3,-2}$
(4, 6)	$\bar{\Phi}_{3,1,1,-\frac{2}{3}} + \bar{\Phi}_{1,1,3,-2} + \Phi_{1,3,1,0} + 2\Phi_{1,2,2,0} + \Phi_{8,1,1,0} + \Phi_{3,1,1,-\frac{2}{3}} + \Phi_{1,1,3,-2}$
(4, 7)	$\bar{\Phi}_{1,1,2,-1} + 2\bar{\Phi}_{1,1,1,2} + \bar{\Phi}_{3,1,1,-\frac{2}{3}} + \Phi_{1,1,2,-1} + \Phi_{1,1,3,0} + 4\Phi_{1,2,2,0} + \Phi_{8,1,1,0} + 2\Phi_{1,1,1,2} + \Phi_{3,1,1,-\frac{2}{3}}$
(4, 8)	$2\bar{\Phi}_{1,1,2,-1} + \bar{\Phi}_{1,1,1,2} + \bar{\Phi}_{3,1,1,-\frac{2}{3}} + 2\Phi_{1,1,2,-1} + \Phi_{1,1,3,0} + 4\Phi_{1,2,2,0} + \Phi_{8,1,1,0} + \Phi_{1,1,1,2} + \Phi_{3,1,1,-\frac{2}{3}}$
(4, 9)	$\bar{\Phi}_{1,1,2,-1} + \bar{\Phi}_{1,1,1,2} + \bar{\Phi}_{3,1,1,-\frac{2}{3}} + \Phi_{1,1,2,-1} + 2\Phi_{1,1,3,0} + 4\Phi_{1,2,2,0} + \Phi_{8,1,1,0} + \Phi_{1,1,1,2} + \Phi_{3,1,1,-\frac{2}{3}}$
(4, 10)	$2\bar{\Phi}_{1,1,2,-1} + \bar{\Phi}_{3,1,1,-\frac{2}{3}} + 2\Phi_{1,1,2,-1} + 2\Phi_{1,1,3,0} + 4\Phi_{1,2,2,0} + \Phi_{8,1,1,0} + \Phi_{3,1,1,-\frac{2}{3}}$
(4, 11)	$\bar{\Phi}_{1,1,2,-1} + \bar{\Phi}_{3,1,1,-\frac{2}{3}} + \Phi_{1,1,2,-1} + 3\Phi_{1,1,3,0} + 4\Phi_{1,2,2,0} + \Phi_{8,1,1,0} + \Phi_{3,1,1,-\frac{2}{3}}$
(5, 1)	$\bar{\Phi}_{1,2,1,1} + \bar{\Phi}_{1,1,2,-1} + 5\bar{\Phi}_{1,1,1,2} + 2\bar{\Phi}_{3,1,1,-\frac{2}{3}} + \Phi_{1,2,1,1} + \Phi_{1,1,2,-1} + 2\Phi_{1,3,1,0} + \Phi_{8,1,1,0} + 5\Phi_{1,1,1,2} + 2\Phi_{3,1,1,-\frac{2}{3}}$
(5, 2)	$\bar{\Phi}_{1,1,2,-1} + 5\bar{\Phi}_{1,1,1,2} + 2\bar{\Phi}_{3,1,1,-\frac{2}{3}} + \Phi_{1,1,2,-1} + 2\Phi_{1,3,1,0} + \Phi_{1,2,2,0} + \Phi_{8,1,1,0} + 5\Phi_{1,1,1,2} + 2\Phi_{3,1,1,-\frac{2}{3}}$
(5, 3)	$2\bar{\Phi}_{1,1,2,-1} + 4\bar{\Phi}_{1,1,1,2} + 2\bar{\Phi}_{3,1,1,-\frac{2}{3}} + 2\Phi_{1,1,2,-1} + 2\Phi_{1,3,1,0} + \Phi_{1,2,2,0} + \Phi_{8,1,1,0} + 4\Phi_{1,1,1,2} + 2\Phi_{3,1,1,-\frac{2}{3}}$
(5, 4)	$\bar{\Phi}_{1,2,1,1} + \bar{\Phi}_{1,1,1,2} + 2\bar{\Phi}_{3,1,1,-\frac{2}{3}} + \bar{\Phi}_{1,1,3,-2} + \Phi_{1,2,1,1} + 2\Phi_{1,3,1,0} + \Phi_{8,1,1,0} + \Phi_{1,1,1,2} + 2\bar{\Phi}_{3,1,1,-\frac{2}{3}} + \Phi_{1,1,3,-2}$
(5, 5)	$\bar{\Phi}_{1,1,1,2} + 2\bar{\Phi}_{3,1,1,-\frac{2}{3}} + \bar{\Phi}_{1,1,3,-2} + 2\Phi_{1,3,1,0} + \Phi_{1,2,2,0} + \Phi_{8,1,1,0} + \Phi_{1,1,1,2} + 2\bar{\Phi}_{3,1,1,-\frac{2}{3}} + \Phi_{1,1,3,-2}$
(5, 6)	$\bar{\Phi}_{1,1,2,-1} + 2\bar{\Phi}_{3,1,1,-\frac{2}{3}} + \bar{\Phi}_{1,1,3,-2} + \Phi_{1,1,2,-1} + 2\Phi_{1,3,1,0} + \Phi_{1,2,2,0} + \Phi_{8,1,1,0} + 2\bar{\Phi}_{3,1,1,-\frac{2}{3}} + \Phi_{1,1,3,-2}$
(5, 7)	$2\bar{\Phi}_{3,1,1,-\frac{2}{3}} + \bar{\Phi}_{1,1,3,-2} + \Phi_{1,3,1,0} + 3\Phi_{1,2,2,0} + \Phi_{8,1,1,0} + 2\bar{\Phi}_{3,1,1,-\frac{2}{3}} + \Phi_{1,1,3,-2}$
(5, 8)	$\bar{\Phi}_{3,1,2,\frac{1}{3}} + \bar{\Phi}_{1,1,3,-2} + 2\Phi_{1,3,1,0} + \Phi_{1,2,2,0} + \Phi_{8,1,1,0} + \Phi_{3,1,2,\frac{1}{3}} + \Phi_{1,1,3,-2}$
(5, 9)	$2\bar{\Phi}_{1,1,2,-1} + \bar{\Phi}_{1,1,1,2} + 2\bar{\Phi}_{3,1,1,-\frac{2}{3}} + 2\Phi_{1,1,2,-1} + \Phi_{1,1,3,0} + 5\Phi_{1,2,2,0} + \Phi_{8,1,1,0} + \Phi_{1,1,1,2} + 2\bar{\Phi}_{3,1,1,-\frac{2}{3}}$
(5, 10)	$\bar{\Phi}_{1,1,2,-1} + \bar{\Phi}_{1,1,1,2} + 2\bar{\Phi}_{3,1,1,-\frac{2}{3}} + \Phi_{1,1,2,-1} + 2\Phi_{1,1,3,0} + 5\Phi_{1,2,2,0} + \Phi_{8,1,1,0} + \Phi_{1,1,1,2} + 2\bar{\Phi}_{3,1,1,-\frac{2}{3}}$
(5, 11)	$2\bar{\Phi}_{1,1,2,-1} + 2\bar{\Phi}_{3,1,1,-\frac{2}{3}} + 2\Phi_{1,1,2,-1} + 2\Phi_{1,1,3,0} + 5\Phi_{1,2,2,0} + \Phi_{8,1,1,0} + 2\bar{\Phi}_{3,1,1,-\frac{2}{3}}$
(5, 12)	$\bar{\Phi}_{1,1,2,-1} + 2\bar{\Phi}_{3,1,1,-\frac{2}{3}} + \Phi_{1,1,2,-1} + 3\Phi_{1,1,3,0} + 5\Phi_{1,2,2,0} + \Phi_{8,1,1,0} + 2\bar{\Phi}_{3,1,1,-\frac{2}{3}}$
(5, 13)	$\bar{\Phi}_{1,1,2,-1} + \bar{\Phi}_{3,1,2,\frac{1}{3}} + \Phi_{1,1,2,-1} + 2\Phi_{1,1,3,0} + 5\Phi_{1,2,2,0} + \Phi_{8,1,1,0} + \Phi_{3,1,2,\frac{1}{3}}$

Not all the fields in Table IV can lead to valid configurations. The fields which never give an anomaly-free configuration are  $\Phi_{8,2,2,0}$ ,  $\Phi_{3,2,2,\frac{4}{3}}$ ,  $\Phi_{3,3,1,-\frac{2}{3}}$ ,  $\Phi_{3,1,3,-\frac{2}{3}}$ ,  $\Phi_{6,3,1,\frac{2}{3}}$ ,  $\Phi_{6,1,3,\frac{2}{3}}$  and  $\Phi_{1,3,3,0}$ . Also the field  $\Phi_{3,2,2,-\frac{2}{3}}$  appears only exactly once in the variant (5, 5) in the configuration  $4\Phi_{1,2,1,1} + \Phi_{3,1,1,-\frac{2}{3}} + \Phi_{3,2,2,-\frac{2}{3}} + 4\Phi_{1,1,2,1} + 2\Phi_{1,1,1,2} + 5\Phi_{3,1,1,-\frac{2}{3}}$ . Note that the example configurations we give for the variants (1, 3) and (1, 4) are not the model II and model I discussed in Ref. [20].

Many of the 53 variants have only configurations with  $\Phi_{1,1,2,-1}$  (and conjugate) for the breaking of the LR symmetry. These variants need either the presence of  $\Phi_{1,3,1,0}$  [as for example in the configuration shown for variant (2, 1)] or  $\Phi_{1,1,3,0}$  [see, for example, (1, 4)] or an additional singlet  $\Phi_{1,1,1,0}$  (not shown, since it has no contribution to any  $\Delta b_i^{LR}$ ) to generate seesaw neutrino masses. Using the  $\Phi_{1,1,1,0}$  one could construct either an inverse [32] or a linear [33,34] seesaw mechanism, while with  $\Phi_{1,3,1,0}$  a seesaw type III [35] is a possibility and, finally, a  $\Phi_{1,1,3,0}$  allows for an inverse seesaw type III [20]. The first example where a

valid configuration with  $\Phi_{1,1,3,-2}$  appears is the variant (3, 4). The simplest configuration is  $\Phi_{1,2,1,1} + \Phi_{1,3,1,0} + \Phi_{8,1,1,0} + \Phi_{1,1,3,-2} + \bar{\Phi}_{1,2,1,1} + \bar{\Phi}_{1,1,3,-2}$  (not the example given in Table I). The VEV of the  $\Phi_{1,1,3,-2}$  does not only break the LR symmetry, it can also generate a Majorana mass term for the right-handed neutrino fields, i.e., configurations with  $\Phi_{1,1,3,-2}$  can generate a seesaw type I, in principle. Finally, the simplest possibility with a valid configuration including  $\Phi_{1,3,1,-2}$  is found in variant (4, 1) with  $\Phi_{1,1,2,-1} + \Phi_{8,1,1,0} + \Phi_{1,1,1,2} + \Phi_{3,1,1,\frac{4}{3}} + \Phi_{1,3,1,-2} + \bar{\Phi}_{1,1,2,-1} + \bar{\Phi}_{1,1,1,2} + \bar{\Phi}_{3,1,1,\frac{4}{3}} + \bar{\Phi}_{1,3,1,-2}$ . The presence of  $\Phi_{1,3,1,-2}$  allows us to generate a seesaw type II for the neutrinos.

As mentioned in the introduction, it is not possible to construct a sliding scale model in which the LR symmetry is broken by two pairs of triplets:  $\Phi_{1,3,1,-2} + \bar{\Phi}_{1,3,1,-2} + \Phi_{1,1,3,-2} + \bar{\Phi}_{1,1,3,-2}$ . The sum of the  $\Delta b$ 's for these fields adds up to  $(\Delta b_3^{LR}, b_L^{LR}, \Delta b_R^{LR}, \Delta b_{B-L}^{LR}) = (0, 4, 4, 18)$ . This leaves only the possibilities (4, 4), (5, 4), (5, 5), etc. from Table II. However, the largest  $\Delta b_{B-L}^{LR}$  of these models is

(5, 4) which allows for  $\Delta b_{B-L}^{\text{LR}} = 31/2$ , smaller than the required 18. This observation is consistent with the analysis done in Ref. [19], where the authors have shown that a supersymmetric LR-symmetric model, where the LR symmetry is broken by two pairs of triplets, requires a minimal LR scale of at least  $10^9$  GeV (and, actually, a much larger scale in minimal renormalizable models, if GUT-scale thresholds are small).

A few final comments on the variants with  $\Delta b_2^{\text{LR}} = \Delta b_3^{\text{LR}} = 0$ . Strictly speaking, none of these variants is guaranteed to give a valid model in the sense defined in Sec. II A, since they contain only one  $\Phi_{1,2,2,0} \rightarrow (H_u, H_d)$  and no vectorlike quarks (no  $\Phi_{3,1,1,\frac{4}{3}}$  or  $\Phi_{3,1,1,-\frac{2}{3}}$ ). With such a minimal configuration the Cabbibo-Kobayashi-Maskawa (CKM) matrix is trivial at the energy scale where the LR symmetry is broken. We nevertheless list these variants, since in principle a CKM matrix for quarks consistent with experimental data could be generated at 1-loop level from flavor violating soft terms, as discussed in Ref. [36].

Before we end this section let us mention that variants with  $\Delta b_3^{\text{LR}} = 5$  will not be testable at LHC by measurements of soft SUSY breaking mass terms (“invariants”). This is discussed below in Sec. III A.

### C. Model class II: Additional intermediate Pati-Salam scale

In the second class of supersymmetric  $SO(10)$ -inspired models we consider,  $SO(10)$  is broken first to the Pati-Salam (PS) group. The complete breaking chain thus is

$$\begin{aligned} SO(10) &\rightarrow SU(4) \times SU(2)_L \times SU(2)_R \\ &\rightarrow SU(3)_c \times SU(2)_L \times SU(2)_R \times U(1)_{B-L} \\ &\rightarrow \text{MSSM}. \end{aligned} \quad (8)$$

The representations available from the decomposition of  $SO(10)$  multiplets up to **126** are listed in Table V in the Appendix, together with their possible  $SO(10)$  origin. Breaking  $SO(10)$  to the PS group requires that  $\Psi_{1,1,1}$  from the **54** takes a VEV. The subsequent breaking of the PS group to the LR group requires that the singlet in  $\Psi_{15,1,1}$ , originally from the **45** of  $SO(10)$ , acquires a VEV. And, finally, as before in the LR class, the breaking of LR to  $SU(3)_c \times SU(2)_L \times U(1)_Y$  can be done either via  $\Phi_{1,1,2,-1}$  or  $\Phi_{1,1,3,-2}$  (and/or conjugates).

The additional  $b_i$  coefficients for the regime  $[m_{\text{PS}}, m_{\text{GUT}}]$  are given by

$$(b_4^{\text{PS}}, b_2^{\text{PS}}, b_R^{\text{PS}}) = (-6, 1, 1) + (\Delta b_4^{\text{PS}}, \Delta b_2^{\text{PS}}, \Delta b_R^{\text{PS}}), \quad (9)$$

where, as before, the  $\Delta b_i^{\text{PS}}$  include contributions from superfields not part of the MSSM field content.

In this class of models, the unification scale is independent of the LR one if the following condition is satisfied:

$$\begin{aligned} 0 &= \left( \Delta b_3^{\text{LR}} - \Delta b_2^{\text{LR}}, \frac{3}{5} \Delta b_R^{\text{LR}} + \frac{2}{5} \Delta b_{B-L}^{\text{LR}} - \Delta b_2^{\text{LR}} - \frac{18}{5} \right) \\ &\cdot \begin{pmatrix} 2 & 3 \\ -5 & 0 \end{pmatrix} \cdot \begin{pmatrix} \Delta b_4^{\text{PS}} - \Delta b_2^{\text{PS}} - 3 \\ \Delta b_R^{\text{PS}} - \Delta b_2^{\text{PS}} - 12 \end{pmatrix}. \end{aligned} \quad (10)$$

It is worth noting that requiring also that  $m_{\text{PS}}$  is independent of the LR scale would lead to the conditions in Eq. (7), which are the sliding conditions for LR models. We can see that this must be so in the following way: for some starting values at  $m_{\text{PS}}$  of the three gauge couplings, the scales  $m_{\text{PS}}$  and  $m_G$  can be adjusted such that the two splittings between the three gauge couplings are reduced to zero at  $m_G$ . This fixes these scales, which must not change even if  $m_R$  is varied. As such  $\alpha_3^{-1}(m_{\text{PS}}) - \alpha_2^{-1}(m_{\text{PS}})$  and  $\alpha_3^{-1}(m_{\text{PS}}) - \alpha_R^{-1}(m_{\text{PS}})$  are also fixed and they can be determined by running the MSSM up to  $m_{\text{PS}}$ . The situation is therefore equal to the one that lead to the equalities in Eq. (7), namely the splittings between the gauge couplings at some fixed scale must be independent of  $m_R$ .

Since there are now two unknown scales involved in the problem, the maximum  $\Delta b_i^X$  allowed by perturbativity in one regime do not only depend on the new scale  $X$ , but also on the  $\Delta b_i^Y$  in the other regime as well. As an example, in Fig. 3 we show the  $\text{Max}(\Delta b_4^{\text{PS}})$  allowed by  $\alpha_G^{-1} \geq 0$  for different values of  $\Delta b_3^{\text{LR}}$  and for the choices  $m_R = 1$  TeV and  $m_G = 10^{16}$  GeV. The dependence of  $\text{Max}(\Delta b_4^{\text{PS}})$  on  $m_R$  is rather weak, as long as  $m_R$  does not approach the GUT scale.

If we impose the limits  $m_R = 10^3$  GeV,  $m_{\text{PS}} \leq 10^6$  GeV and take  $m_G = 10^{16}$  GeV, the bounds for the different  $\Delta b$ 's can be written as<sup>7</sup>

$$\Delta b_2^{\text{PS}} + \frac{3}{10} \Delta b_2^{\text{LR}} < 7.2, \quad (11)$$

$$\Delta b_4^{\text{PS}} + \frac{3}{10} \Delta b_3^{\text{LR}} < 10, \quad (12)$$

$$\frac{2}{5} \Delta b_4^{\text{PS}} + \frac{3}{5} \Delta b_R^{\text{PS}} + \frac{3}{10} \left( \frac{2}{5} \Delta b_{B-L}^{\text{LR}} + \frac{3}{5} \Delta b_R^{\text{LR}} \right) < 17. \quad (13)$$

However, as Fig. 3 shows,  $\text{Max}(\Delta b_4^{\text{PS}})$  is a rather strong function of the choice of  $\Delta b_3^{\text{LR}}$ . Note that if  $m_{\text{PS}}$  is low, say below  $10^{10}$  GeV, larger  $\Delta b_3^{\text{LR}}$ 's are possible, up to  $\Delta b_3^{\text{LR}} = 7$ ; see Fig. 3. The large values of  $\text{Max}(\Delta b^{\text{LR}})$  and  $\text{Max}(\Delta b^{\text{PS}})$  allow, in principle, a huge number of variants to be constructed in class II. This is demonstrated in Fig. 4, where we show the number of variants for an

<sup>7</sup>In fact, the bounds shown here exclude a few variants with  $m_{\text{PS}} < 10^6$  GeV. This is because of the following: while in most cases the most conservative assumption is to assume that  $m_{\text{PS}}$  is as large as possible ( $= 10^6$  GeV; this leads to a smaller running in the PS regime) in deriving these bounds, there are some cases where this is not true. This is a minor complication which nonetheless was taken into account in our computations.

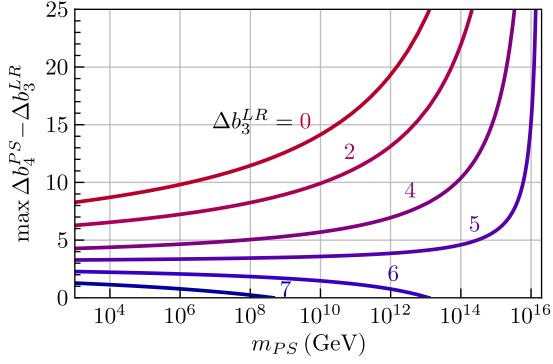


FIG. 3 (color online). Maximum value of  $\Delta b_4^{PS} - \Delta b_3^{LR}$  allowed by perturbativity as function of the scale  $m_{PS}$  in GeV. The different lines have been calculated for six different values of  $\Delta b_3^{LR}$ . The plot assumes that  $m_R = 1$  TeV. The line near the bottom corresponds to  $\Delta b_3^{LR} = 7$ .

assumed  $m_R \sim 1$  TeV as a function of the scale  $m_{PS}$ . Up to  $m_{PS} = 10^{15}$  GeV the list is exhaustive. For larger values of  $m_{PS}$  we have only scanned a finite (though large) set of possible variants. Note that these are variants, not configurations. As in the case of class I practically any variant can be made by several possible anomaly-free configurations. The exhaustive list of variants ( $m_{PS} = 10^{15}$  GeV) contains a total of 105909 possibilities and can be found in Ref. [31].

With such a huge number of possible variants, we can discuss only some general features here. First of all, within the exhaustive set up to  $m_{PS} = 10^{15}$  GeV, there are a total of 1570 different sets of  $\Delta b_i^{LR}$ , each of which can be completed by more than one set of  $\Delta b_i^{PS}$ . Variants with the same set of  $\Delta b_i^{LR}$  but different completion of  $\Delta b_i^{PS}$  have, of course, the same configuration in the LR regime, but come with a different value for  $m_{PS}$  for fixed  $m_R$ . Thus, they have in general different values for  $\alpha_{B-L}$  and  $\alpha_R$  at the LR scale and (see next section) different values of the invariants. For example, for the smallest values of  $\Delta b_i^{LR}$  that are possible in principle [ $\Delta b_i^{LR} = (0, 0, 1, 3/2)$ ], there are 342 different completing sets of  $\Delta b_i^{PS}$ .

The very simplest set of  $\Delta b_i^{LR}$  possible,  $\Delta b_i^{LR} = (0, 0, 1, 3/2)$ , corresponds to the configuration  $\Phi_{1,1,2,-1} + \bar{\Phi}_{1,1,2,-1}$ . These fields are necessary to break  $SU(2)_R \times U(1)_{B-L} \rightarrow U(1)_Y$ . Their presence in the LR regime requires that in the PS regime we have at least one set of copies of  $\Psi_{4,1,2} + \bar{\Psi}_{4,1,2}$ . In addition, for breaking the PS group to the LR group, we need at least one copy of  $\Psi_{15,1,1}$ . However, the set of  $\Psi_{4,1,2} + \bar{\Psi}_{4,1,2} + \Psi_{15,1,1}$  is not sufficient to generate a sliding scale mechanism and the simplest configuration that can do so, consistent with  $\Delta b_i^{LR} = (0, 0, 1, 3/2)$ , is  $3\Psi_{1,2,2} + 4\Psi_{1,1,3} + \Psi_{4,1,2} + \bar{\Psi}_{4,1,2} + \Psi_{15,1,1}$ , leading to  $\Delta b_i^{PS} = (6, 3, 15)$  and a very low possible value of  $m_{PS}$  of  $m_{PS} = 8.2$  TeV for  $m_R = 1$  TeV (see, however, the discussion on leptoquarks below). The next possible completion for  $\Phi_{1,1,2,-1} + \bar{\Phi}_{1,1,2,-1}$  is  $3\Psi_{1,2,2} + 5\Psi_{1,1,3} + \Psi_{4,1,2} + \bar{\Psi}_{4,1,2} + \Psi_{15,1,1}$ , with  $\Delta b_i^{PS} = (6, 3, 17)$  and  $m_{PS} = 1.3 \times 10^8$  GeV (for  $m_R = 1$  TeV), etc.

As noted already in Sec. II B, one copy of  $\Phi_{1,2,2,0}$  is not sufficient to produce a realistic CKM matrix at tree level. Thus, the minimal configuration of  $\Phi_{1,1,2,-1} + \bar{\Phi}_{1,1,2,-1}$  relies on the possibility of generating all of the departure of the CKM matrix from unity by flavor violating soft masses [36]. There are at least two possibilities to generate a nontrivial CKM at tree level, either by adding (a) another  $\Phi_{1,2,2,0}$  plus (at least) one copy of  $\Phi_{1,1,3,0}$  or via (b) one copy of “vectorlike quarks”  $\Phi_{3,1,1,\frac{4}{3}}$  or  $\Phi_{3,1,1,-\frac{2}{3}}$ . Consider the configuration  $\Phi_{1,1,2,-1} + \bar{\Phi}_{1,1,2,-1} + \Phi_{1,2,2,0} + \Phi_{1,1,3,0}$  first. It leads to  $\Delta b_i^{LR} = (0, 1, 4, 3/2)$ . Since  $\Phi_{1,2,2,0}$  and  $\Phi_{1,1,3,0}$  must come from  $\Psi_{1,2,2}$  (or  $\Psi_{15,2,2}$ ) and  $\Psi_{1,1,3}$ , respectively, the simplest completion for this set of  $\Delta b_i^{LR}$  is again  $3\Psi_{1,2,2} + 4\Psi_{1,1,3} + \Psi_{4,1,2} + \bar{\Psi}_{4,1,2} + \Psi_{15,1,1}$ , leading to  $\Delta b_i^{PS} = (6, 3, 15)$  and value of  $m_{PS}$  of, in this case,  $m_{PS} = 5.4$  TeV for  $m_R = 1$  TeV. Again, many completions with different  $\Delta b_i^{PS}$ 's exist for this set of  $\Delta b_i^{LR}$ .

The other possibility for generating CKM at tree level, adding for example a pair of  $\Phi_{3,1,1,-\frac{2}{3}} + \bar{\Phi}_{3,1,1,-\frac{2}{3}}$ , has

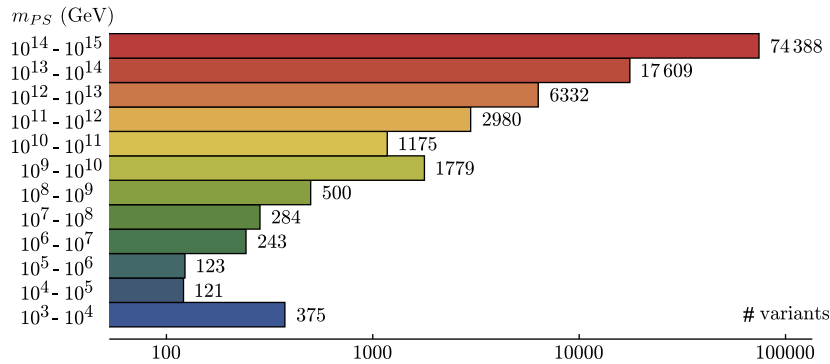


FIG. 4 (color online). The number of possible variants in model class II, assuming  $m_R$  is of order  $m_R \approx 1$  TeV as a function of  $m_{PS}$ . Up to  $m_{PS} = 10^{15}$  GeV the list is exhaustive. For larger values of  $m_{PS}$  we have only scanned a finite (though large) set of possible variants.



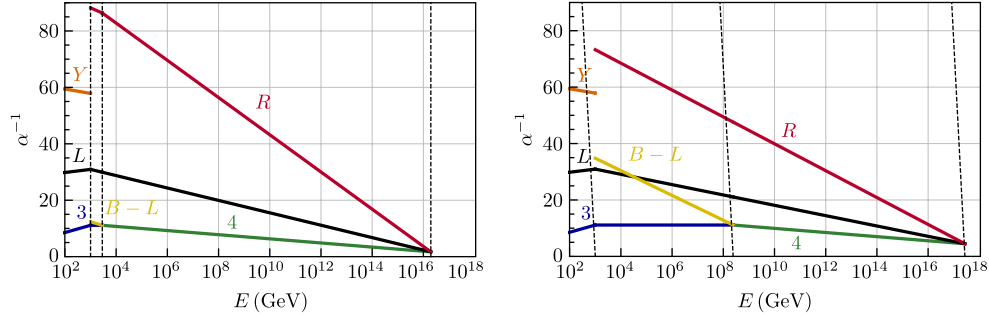


FIG. 5 (color online). Gauge coupling unification for PS models with  $m_R = 10^3$  GeV. In the plot to the left  $(\Delta b_3^{\text{LR}}, \Delta b_L^{\text{LR}}, \Delta b_R^{\text{LR}}, \Delta b_{B-L}^{\text{LR}}, \Delta b_4^{\text{PS}}, \Delta b_L^{\text{PS}}, \Delta b_R^{\text{PS}}) = (3, 5, 10, 3/2, 8, 5, 17)$ , while the plot to the right corresponds to  $\Delta b^{\text{PS}} = (3, 4, 12, 6, 8, 4, 12)$ .

$\Delta b_i^{\text{LR}} = (1, 0, 1, 5/2)$  and its simplest PS completion is  $4\Psi_{1,2,2} + 4\Psi_{1,1,3} + \Psi_{4,1,2} + \bar{\Psi}_{4,1,2} + \Psi_{6,1,1} + \Psi_{15,1,1}$ , with  $\Delta b_i^{\text{PS}} = (7, 4, 16)$  and a  $m_{\text{PS}} = 4.6 \times 10^6$  TeV for  $m_R = 1$  TeV. Also in this case one can find sets with very low values of  $m_{\text{PS}}$ . For example, adding a  $\Phi_{1,2,2,0}$  to this LR configuration [for a  $\Delta b_i^{\text{LR}} = (1, 1, 2, 5/2)$ ], one finds that with the same  $\Delta b_i^{\text{PS}}$  now a value of  $m_{\text{PS}}$  as low as  $m_{\text{PS}} = 8.3$  TeV for  $m_R = 1$  TeV is possible.

We note in passing that the original PS-class model of Ref. [20] in our notation corresponds to  $\Delta b_i^{\text{LR}} = (1, 2, 10, 4)$  and  $\Phi_{1,1,2,-1} + \bar{\Phi}_{1,1,2,-1} + \Phi_{1,2,1,1} + \bar{\Phi}_{1,2,1,1} + \Phi_{1,2,2,0} + 4\Phi_{1,1,3,0} + \Phi_{3,1,1,-\frac{2}{3}} + \bar{\Phi}_{3,1,1,-\frac{2}{3}}$ , completed by  $\Delta b_i^{\text{PS}} = (9, 5, 13)$  with  $\Psi_{4,1,2} + \bar{\Psi}_{4,1,2} + \Psi_{4,2,1} + \Psi_{4,2,1} + \Psi_{1,2,2} + 4\Psi_{1,1,3} + \Psi_{6,1,1} + \Psi_{15,1,1}$ . The lowest possible  $m_{\text{PS}}$  for a  $m_R = 1$  TeV is  $m_{\text{PS}} = 2.4 \times 10^8$  GeV. Obviously this example is not the simplest construction in class II. We also mention that while for the  $\beta$  coefficients it does not make any difference, the superfield  $\Phi_{1,1,3,0}$  can be either interpreted as ‘‘Higgs’’ or as ‘‘matter.’’ In the original construction [20] this ‘‘arbitrariness’’ was used to assign the four copies of  $\Phi_{1,1,3,0}$  to one copy of  $\Omega^c = \Phi_{1,1,3,0}$ ,<sup>8</sup> i.e., Higgs and three copies of  $\Sigma^c = \bar{\Phi}_{1,1,3,0}$ , i.e., matter. In this way  $\Omega^c$  can be used to generate the CKM matrix at tree level (together with the extra bidoublet  $\Phi_{1,2,2,0}$ ), while the  $\Sigma^c$  can be used to generate an inverse seesaw type III for neutrino masses.

As Fig. 4 shows, there are more than 600 variants in which  $m_{\text{PS}}$  can, in principle, be lower than  $m_{\text{PS}} = 10^3$  TeV. Such low PS scales, however, are already constrained by searches for rare decays, such as  $B_s \rightarrow \mu^+ \mu^-$ . This is because the  $\Psi_{15,1,1}$ , which must be present in all our constructions for the breaking of the PS group, contains two leptoquark states. We will not study in detail leptoquark phenomenology [37] here, but mention that in the recent paper [38] absolute lower bounds on leptoquarks within PS models of the order of  $m_{\text{PS}} \approx 40$  TeV have been derived. There are 426 variants for which we find  $m_{\text{PS}}$

lower than this bound, if we put  $m_R$  to 1 TeV. Due to the sliding scale nature of our construction this, of course, does not mean that these models are ruled out by the lower limit found in Ref. [38]. Instead, for these models one can calculate a lower limit on  $m_R$  from the requirement that  $m_{\text{PS}} = 40$  TeV. Depending on the model, lower limits on  $m_R$  between  $m_R = [1.3, 27.7]$  TeV are found for the 426 variants from this requirement.

Two example solutions can be seen in Fig. 5. We have chosen one example with a very low  $m_{\text{PS}}$  (left) and one with an intermediate  $m_{\text{PS}}$  (right). Note that different from the class-I models, in the class-II models the GUT scale is no longer fixed to the MSSM value  $m_G \approx 2 \times 10^{16}$  GeV. Our samples are restricted to variants which have  $m_G$  in the interval  $[10^{16}, 10^{18}]$  GeV.

#### D. Models with an $U(1)_R \times U(1)_{B-L}$ intermediate scale

Finally, we consider models where there is an additional intermediate symmetry  $U(1)_R \times U(1)_{B-L}$  that follows the stage  $SU(2)_R \times U(1)_{B-L}$ . The field content relevant to this model is specified in Table VI of the Appendix. In this case the original  $SO(10)$  is broken down to the MSSM in three steps,

$$\begin{aligned} SO(10) &\rightarrow SU(3)_c \times SU(2)_L \times SU(2)_R \times U(1)_{B-L} \\ &\rightarrow SU(3)_c \times SU(2)_L \times U(1)_R \times U(1)_{B-L} \\ &\rightarrow \text{MSSM}. \end{aligned} \quad (14)$$

The first step is achieved in the same way as in class-I models. The subsequent breaking  $SU(2)_R \times U(1)_{B-L} \rightarrow U(1)_R \times U(1)_{B-L}$  is triggered by  $\Phi_5 = \Phi_{1,1,3,0}$  and the last one requires  $\Phi'_4 = \Phi'_{1,1,\frac{1}{2},-1}$ ,  $\Phi'_{20} = \Phi'_{1,1,1,-2}$  or their conjugates.

In theories with more than one  $U(1)$  gauge factor, the 1-loop evolution of the gauge couplings and soft SUSY breaking terms are affected by the extra kinetic mixing terms. The couplings are defined by the matrix

$$G = \begin{pmatrix} g_{RR} & g_{RX} \\ g_{XR} & g_{XX} \end{pmatrix} \quad (15)$$

<sup>8</sup>The original paper [20] called this field  $\Omega$ . However, in our notation it would be natural to call  $\Omega = \Phi_{1,3,1,0}$ .

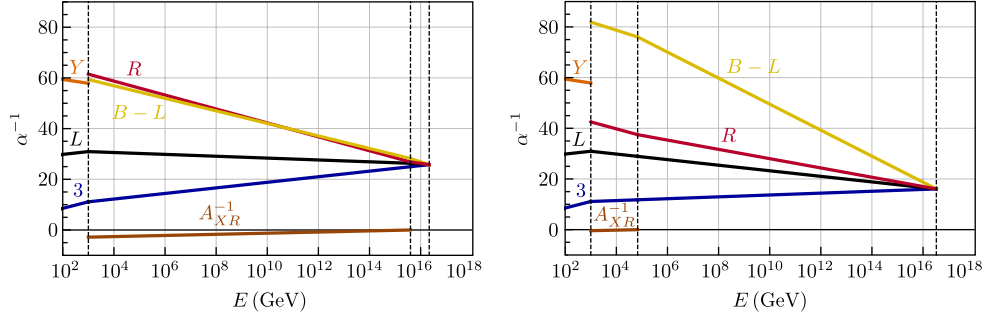


FIG. 6 (color online). Gauge coupling unification in models with an  $U(1)_R \times U(1)_{B-L}$  intermediate scale, for  $m_R = 10^3$  GeV. Left:  $(\Delta b_3^{\text{LR}}, \Delta b_L^{\text{LR}}, \Delta b_R^{\text{LR}}, \Delta b_{B-L}^{\text{LR}}, \Delta b_3^{B-L}, \Delta b_L^{B-L}, \Delta \gamma_{RR}, \Delta \gamma_{XR}, \Delta \gamma_{XX}) = (0, 1, 3, 3, 0, 0, 1/2, -\sqrt{3}/8, 3/4)$ . Right:  $(2, 2, 4, 8, 2, 2, 1/2, -\sqrt{3}/8, 11/4)$ . The line, which appears close to zero in the  $U(1)_R \times U(1)_{B-L}$  regime, is the running of the off-diagonal element of the matrix  $A^{-1}$ ; i.e., it measures the size of the  $U(1)$  mixing in the model.

and  $A(t) = (GG^T)/(4\pi) = (A^{-1}(t_0) - \gamma(t-t_0))^{-1}$ , where  $t = \frac{1}{2\pi} \log(\frac{\mu}{\mu_0})$  [20]. Here,  $\mu$  and  $\mu_0$  stand for the energy scale and its normalization point and  $A$  is the generalization of  $\alpha$  to matrix form. The matrix of anomalous dimension,  $\gamma$ , is defined by the charges of each chiral superfield  $f$  under  $U(1)_R$  and  $U(1)_{B-L}$ :

$$\gamma = \sum_f Q_f Q_f^T, \quad (16)$$

where  $Q_f$  denotes a column vector of those charges. Taking the MSSM's field content we find

$$\gamma = \begin{pmatrix} 7 & 0 \\ 0 & 6 \end{pmatrix}. \quad (17)$$

To ensure the canonical normalization of the  $B-L$  charge within the  $SO(10)$  framework,  $\gamma$  should be normalized as  $\gamma^{\text{can}} = N\gamma^{\text{phys}}N$ , where  $N = \text{diag}(1, \sqrt{3/8})$ .

Then, the additional  $\beta$  coefficients for the running step  $[m_{B-L}, m_R]$  are given by

$$(b_3^{B-L}, b_2^{B-L}, \gamma_{RR}^{B-L}, \gamma_{XR}^{B-L}, \gamma_{XX}^{B-L}) = (-3, 1, 6, 0, 7) + (\Delta b_3^{B-L}, \Delta b_2^{B-L}, \Delta \gamma_{RR}, \Delta \gamma_{XR}, \Delta \gamma_{XX}). \quad (18)$$

As in the previous PS case, we consider  $m_{B-L} = 10^3$  GeV,  $m_G \geq 10^{16}$  GeV and  $m_R \leq 10^6$  GeV. Taking into account the matching condition

$$p_Y^T \cdot A^{-1}(m_{B-L}) \cdot p_Y = \alpha_1^{-1}(m_{B-L}) \quad (19)$$

and  $p_Y^T = (\sqrt{\frac{3}{5}}, \sqrt{\frac{2}{5}})$ , the bounds on the  $\Delta b$  are

$$\Delta b_2^{\text{LR}} + \frac{3}{10} \Delta b_2^{B-L} < 7.1, \quad \Delta b_3^{\text{LR}} + \frac{3}{10} \Delta b_3^{B-L} < 6.9, \\ \frac{3}{5} \Delta b_R^{\text{LR}} + \frac{2}{5} \Delta b_{B-L}^{\text{LR}} + \frac{3}{10} p_Y^T \cdot \Delta \gamma \cdot p_Y < 10.8. \quad (20)$$

Even with this restriction in the scales we found 15610 solutions, more than in the PS case, due to the fact that there are more  $\Delta b$ 's that can be varied to obtain solutions.

The qualitative features of the running of the gauge couplings are shown for two examples in Fig. 6. In those two examples the  $(\Delta b_3^{\text{LR}}, \Delta b_L^{\text{LR}}, \Delta b_R^{\text{LR}}, \Delta b_{B-L}^{\text{LR}}, \Delta b_3^{B-L}, \Delta b_L^{B-L}, \Delta \gamma_{RR}, \Delta \gamma_{XR}, \Delta \gamma_{XX})$  have been chosen as  $(0, 1, 3, 3, 0, 0, 1/2, -\sqrt{3}/8, 3/4)$  (left) and  $(2, 2, 4, 8, 2, 2, 1/2, -\sqrt{3}/8, 11/4)$  (right). The former corresponds to the minimal configuration  $\Phi'_{1,1,1/2,-1} + \bar{\Phi}'_{1,1,1/2,-1}$  in the lower regime and  $\Phi_{1,1,2,-1} + \bar{\Phi}_{1,1,2,-1} + \Phi_{1,1,3,0} + \Phi_{1,2,1,1} + \bar{\Phi}_{1,2,1,1}$  in the higher (LR-symmetric regime). The latter corresponds to  $\Phi'_{1,1,1/2,-1} + \bar{\Phi}'_{1,1,1/2,-1} + \Phi'_{1,3,0,0} + 2\Phi'_{3,1,1,-2/3} + 2\bar{\Phi}'_{3,1,1,-2/3}$  and  $2(\Phi_{1,1,2,-1} + \bar{\Phi}_{1,1,2,-1}) + \Phi_{1,1,3,0} + \Phi_{1,3,1,0} + \Phi_{1,1,1,2} + \bar{\Phi}_{1,1,1,2} + 2(\Phi_{3,1,1,-2/3} + \bar{\Phi}_{3,1,1,-2/3})$ , respectively.

For models in this class, the sliding condition requires that the unification scale is independent of  $m_{B-L}$  and this happens when

$$0 = (\Delta b_3^{B-L} - \Delta b_2^{B-L}, p_Y^T \cdot \Delta \gamma \cdot p_Y - \Delta b_2^{B-L}) \cdot \begin{pmatrix} 0 & 1 \\ -1 & 0 \end{pmatrix} \cdot \begin{pmatrix} \Delta b_3^{\text{LR}} - \Delta b_2^{\text{LR}} \\ \frac{3}{5} \Delta b_R^{\text{LR}} + \frac{2}{5} \Delta b_{B-L}^{\text{LR}} - \Delta b_2^{\text{LR}} - \frac{18}{5} \end{pmatrix}. \quad (21)$$

Similarly to PS models, in this class of models the higher intermediate scale ( $m_R$ ) depends, in general, on the lower one ( $m_{B-L}$ ). However, there is also here a special condition which makes both  $m_R$  and  $m_G$  simultaneously independent of  $m_{B-L}$ , which is

$$\Delta b_3^{\text{LR}} = \Delta b_2^{\text{LR}} = p_Y^T \cdot \Delta \gamma \cdot p_Y. \quad (22)$$

Models of this kind are, for example, those with  $\Delta b_3 = 0$  and  $m_R$  large, namely  $m_R \geq 10^{13}$  GeV. One case is given by the model in Ref. [20], where  $m_R \simeq 4 \times 10^{15}$  GeV.

### III. INVARIANTS

#### A. Leading-log RGE invariants

In this section we briefly recall the basic definitions [20] for the calculation of the invariants [25–27]. In mSUGRA

there are four continuous and one discrete parameters: the common gaugino mass  $M_{1/2}$ , the common scalar mass  $m_0$ , the trilinear coupling  $A_0$  and the choice of the sign of the  $\mu$  parameter,  $\text{sgn}(\mu)$ . In addition, the ratio of vacuum expectation values of  $H_d$  and  $H_u$ ,  $\tan \beta = \frac{v_u}{v_d}$ , is a free parameter. The latter is the only one defined at the weak scale, while all the others are assigned a value at the GUT scale.

Gaugino masses scale as gauge couplings do and so the requirement of GCU fixes the gaugino masses at the low scale

$$M_i(m_{\text{SUSY}}) = \frac{\alpha_i(m_{\text{SUSY}})}{\alpha_G} M_{1/2}. \quad (23)$$

Neglecting the Yukawa and soft trilinear couplings for the soft mass parameters of the first two generations of sfermions one can write

$$m_{\tilde{f}}^2 - m_0^2 = \frac{M_{1/2}^2}{2\pi\alpha_G^2} \sum_{R_j} \sum_{i=1}^N c_i^{f,R_j} \alpha_{i-}^{R_j} \alpha_{i+}^{R_j} (\alpha_{i-}^{R_j} + \alpha_{i+}^{R_j}) \log \frac{m_{i+}^{R_j}}{m_{i-}^{R_j}}. \quad (24)$$

Here, the sum over “ $R_j$ ” runs over the different regimes in the models under consideration, while the sum over  $i$  runs over all gauge groups in a given regime.  $m_{i+}^{R_j}$  and  $m_{i-}^{R_j}$  are the upper and lower boundaries of the  $R_j$  regime and  $\alpha_{i+}^{R_j}$ ,  $\alpha_{i-}^{R_j}$  are the values of the gauge coupling of group  $i$ ,  $\alpha_i$ , at these scales. As for the coefficients  $c_i$ , they can be calculated from the quadratic Casimir of representations of each field under each gauge group  $i$  and are given for example in Ref. [20]. In the presence of multiple  $U(1)$  gauge groups the renormalization group equations (RGEs) are different (see for instance Ref. [39] and references contained therein) and this leads to a generalization of Eq. (24) for the  $U(1)$  mixing phase [20]. Here we just quote the end result (with a minor correction to the one shown in this last reference) ignoring the non- $U(1)$  groups:

$$\tilde{m}_{\tilde{f}-}^2 - \tilde{m}_{\tilde{f}+}^2 = \frac{M_{1/2}^2}{\pi\alpha_G^2} Q_f^T A_- (A_- + A_+) A_+ Q_f \log \frac{m_+}{m_-}, \quad (25)$$

where  $m_+$  and  $m_-$  are the boundary scales of the  $U(1)$  mixing regime and  $A_+$ ,  $A_-$  are the  $A$  matrix defined in the previous section (which generalizes  $\alpha$ ) evaluated in these two limits. Likewise,  $\tilde{m}_{\tilde{f}+}^2$  and  $\tilde{m}_{\tilde{f}-}^2$  are the values of the soft mass parameter of the sfermion  $\tilde{f}$  at these two energy scales. The equation above is a good approximation to the result obtained by integration of the following 1-loop RGE for the soft masses which assumes unification of gaugino masses and gauge coupling constants:

$$\frac{d}{dt} \tilde{m}_{\tilde{f}}^2 = - \frac{4M_{1/2}^2}{\alpha_G^2} Q_f^T A^3 Q_f. \quad (26)$$

Note that in the limit where the  $U(1)$  mixing phase extends all the way up to  $m_G$ , the  $A$  matrix measured at different

energy scales will always commute and therefore Eq. (25) presented here matches the one in Ref. [20] and in fact both are exact integrations of (26). However, if this is not the case, it is expected that there will be a small discrepancy between the two approximations, which nevertheless is numerically small and therefore negligible.

From the five soft sfermion mass parameters of the MSSM and one of the gaugino masses it is possible to form four different combinations that, at 1-loop level in the leading-log approximation, do not depend on the values of  $m_0$  and  $M_{1/2}$  and are therefore called invariants:

$$\begin{aligned} LE &= (m_{\tilde{L}}^2 - m_{\tilde{E}}^2)/M_1^2, & QE &= (m_{\tilde{Q}}^2 - m_{\tilde{E}}^2)/M_1^2, \\ DL &= (m_{\tilde{D}}^2 - m_{\tilde{L}}^2)/M_1^2, & QU &= (m_{\tilde{Q}}^2 - m_{\tilde{U}}^2)/M_1^2. \end{aligned} \quad (27)$$

While being pure numbers in the MSSM, invariants depend on the particle content and gauge group in the intermediate stages, as shown by Eq. (24).

We will not discuss errors in the calculation of the invariants in detail; we refer the interested reader to Ref. [20] and for classical  $SU(5)$  based SUSY seesaw models to Refs. [26,27].

We close this subsection by discussing that not all model variants which we presented in Sec. II will be testable by measurements involving invariants at the LHC. According to Baer *et al.* [40] the LHC at  $\sqrt{s} = 14$  TeV will be able to explore SUSY masses up to  $m_{\tilde{g}} \sim 3.2$  TeV (3.6 TeV) for  $m_{\tilde{q}} \approx m_{\tilde{g}}$  and of  $m_{\tilde{g}} \sim 1.8$  TeV (2.3 TeV) for  $m_{\tilde{q}} \gg m_{\tilde{g}}$  with  $300 \text{ fb}^{-1}$  ( $3000 \text{ fb}^{-1}$ ). The LEP limit on the chargino,  $m_{\tilde{\chi}} > 105$  GeV [30], translates into a lower bound for  $M_{1/2}$ , with the value depending on the  $\Delta b$ . For the class-I models with  $\Delta b = 5$  this leads to  $M_{1/2} \gtrsim 1.06$  TeV. One can assume conservatively  $m_0 = 0$  GeV and calculate from this lower bound on  $M_{1/2}$  a lower limit on the expected squark masses in the different variants. All variants with squark masses above the expected reach of the LHC-14 will then not be testable via measurements of the invariants. This discards all models with  $\Delta b = 5$  as untestable unfortunately.

For completeness we mention that if we take the present LHC limit on the gluino,  $m_{\tilde{g}} \gtrsim 1.1$  TeV [41], this will translate into a lower limit  $M_{1/2} \gtrsim 4.31$  TeV for  $\Delta b = 5$ . We have also checked that models with  $\Delta b = 4$  can still have squarks with masses testable at LHC, even for the more recent LHC bound on the gluino mass.

## B. Classification for invariants

For a given model, the invariants defined in Eq. (27) differ from the mSugra values, and the deviations can be either positive or negative once new superfields (and/or gauge groups) are added to the MSSM. The mSugra limit is reached in our models when the intermediate scales are equal to  $m_G$ , but it should be noted that, in general, when there are two intermediate scales, the smallest one

(henceforth called  $m_-$ ) cannot be pushed all the way up to the unification scale. Therefore, in those cases, the invariants measured at the highest possible  $m_-$  are slightly different from the mSugra invariants.

With this in mind, for each variant of our models, we considered whether the invariants for  $\min m_- (= m_{\text{SUSY}})$  are larger or smaller than for  $\max m_-$ , which tends to be within 1 or 2 orders of magnitude of  $m_G$ . With four invariants there are *a priori*  $2^4 = 16$  possibilities, and in Table III each of them is assigned a number.

However, it is easy to demonstrate that not all of the 16-plet sets can be realized in the three classes of models we consider. This can be understood as follows. If all sfermions have a common  $m_0$  at the GUT scale, then one can show that

$$m_E^2 - m_L^2 + m_D^2 - 2m_U^2 + m_Q^2 = 0 \quad (28)$$

holds independent of the energy scale, at which soft masses are evaluated. This relation is general, regardless of the combination of intermediate scales that we may consider and for all gauge groups we consider. It is a straightforward consequence of the charge assignments of the standard model fermions and can be easily checked by calculating the Dynkin coefficients of the  $E$ ,  $L$ ,  $D$ ,  $U$  and  $Q$  representations in the different regimes. In terms of the invariants, this relation becomes

$$QE = DL + 2QU, \quad (29)$$

i.e., only three of the four invariants are independent. From Eq. (29) it is clear that if  $\Delta DL$  and  $\Delta QU$  are both positive (negative), then  $\Delta QE$  must be also positive (negative). This immediately excludes the sets 4, 5, 12 and 13.

Within the MSSM group Eq. (28) allows one relation among the invariants. However, one can calculate the relations among the Dynkin indices of the MSSM sfermions within the extended gauge groups we are considering and in these there is one additional relation:

$$QU = LE. \quad (30)$$

Since Eq. (30) is valid only in the regime(s) with extended gauge group(s), it is not exact, once the running within the MSSM regime is included. However, taking into account the running within the MSSM group one can write

$$QU = LE + f(m_R), \quad (31)$$

with

$$f(m_R) = \frac{2}{33} \left\{ \left[ \frac{33}{10\pi} \alpha_1^{\text{MSSM}} \log \left( \frac{m_R}{m_{\text{SUSY}}} \right) - 1 \right]^2 - 1 \right\}. \quad (32)$$

Here,  $\alpha_1^{\text{MSSM}}$  is the value of  $\alpha_1$  at  $m_{\text{SUSY}}$ . It is easy to see that  $f(m_R)$  is always small ( $< 0.3$ ) and positive and vanishes if  $m_R$  approaches  $m_{\text{SUSY}}$ . Note that here  $m_R$  stands for the scale where the MSSM group is extended; in the class-III models it is therefore  $m_{B-L}$ .

Equation (31) allows us to eliminate three more cases from Table III. Since  $f(m_R)$  is positive,  $\Delta QU \leq \Delta LE$  always, so it is not possible to have  $\Delta LE = -$  and  $\Delta QU = +$ . This excludes three additional sets from Table III: 9, 11 and 15, leaving a total of nine possible sets.

Finally, in class-I models it is possible to eliminate four more sets, namely all of those with  $\Delta DL < 0$ . It is easy to see, with the help of Eq. (24), that this is the case. It follows from the fact that in the LR case, the  $c_i^L$  are nonzero for  $U(1)_{B-L}$  and  $SU(2)_L$  with the values  $3/4$  and  $3/2$ , respectively. Since also the sum is smaller than the  $c_3^D$  (and  $\alpha_3$  is larger than the other couplings,  $D$  must run faster than  $L$  in the LR regime.

By the above reasoning set 6 seems to be, in principle, possible in class I, but is not realized in our complete scan. We found a few examples in class II; see below. Due to the (approximate) relation  $QU = LE$  it seems to be a particularly fine-tuned situation. We also note in passing, that in the high-scale seesaw models of type II [26] and seesaw type III [27] with running only within the MSSM group, all invariants run always towards larger values, i.e., only set 1 is realized in this case.

The above discussion serves only as a general classification of the types of sets of invariants that can be realized

TABLE III. The 16-plet different combinations of signs for four invariants. We assign a “+” if the corresponding invariant, when the lowest intermediate scale is set to  $m_{\text{SUSY}}$ , is larger than its value when this scale is maximized, and “-” otherwise. As discussed in the text, only 9 of the 16-plet different sign combinations can be realized in the models we consider. Moreover, for class I only the sets 1, 2, 10 and 14 can be realized; see discussion. For class III we also have found only sets 1, 2, 3, 6, 7, 8, 10 and 14, but here our search was not exhaustive.

Set #	1	2	3	4	5	6	7	8	9	10	11	12	13	14	15	16
$\Delta LE$	+	+	+	+	+	+	+	+	-	-	-	-	-	-	-	-
$\Delta QE$	+	+	+	-	+	-	-	-	+	+	+	-	+	-	-	-
$\Delta DL$	+	+	-	+	-	+	-	-	+	+	-	+	-	+	-	-
$\Delta QU$	+	-	+	+	-	-	+	-	+	-	+	+	-	-	+	-
Class I?	✓	✓								✓				✓		
Class II?	✓	✓	✓			✓	✓	✓		✓				✓		✓
Class III?	✓	✓	✓			✓	✓	✓		✓				✓		

in the different model classes. The numerical values of the invariants, however, depend on both the variant of the model class and the scale of the symmetry breaking. We will discuss one example for each possible set next.

### C. Invariants in model class I

Figure 7 shows examples of the  $m_R$  dependence of the invariants corresponding to the four cases: sets 1, 2, 10 and 14 of Table III. Note that we have scaled down the invariants  $QE$  and  $DL$  for practical reasons. Note also the different scales in the different plots.

In all cases  $QU \simeq LE$ , if the LR scale extends to very low energies. As explained above, this is a general feature of the extended gauge groups we consider and thus, measuring a nonzero  $QU - LE$  allows us in our setups, in principle, to derive a lower limit on the scale at which the extended gauge group is broken.

Sets 1 and 2 show a quite similar overall behavior in these examples. Set 1, however, can also be found in variants of class I with larger  $\beta$  coefficients, i.e., larger quantitative changes with respect to the mSugra values. It is possible to find variants within class I which fall into set 2, but again due to the required similarity of  $QU$  and  $LE$ , this set can be realized only if both  $QU$  and  $LE$  are numerically very close to their mSugra values. Set 14 in class I, finally, is possible only with  $QE$  and  $DL$  close to their mSugra values, as can be understood from Eq. (29).

In general, for variants with large  $\Delta b_3^{LR}$ , changes in the invariants can be huge; see for example the plot shown for

set 10. The large change is mainly due to the rapid running of the gaugino masses in these variants, but also the sfermion spectrum is very “deformed” with respect to mSugra expectations. For example, a negative  $LE$  means of course that left sleptons are lighter than right sleptons, a feature that can never be found in the “pure” mSugra model. Recall that for solutions with  $\Delta b_3^{LR} = 5$ , the value of the squark masses lies beyond the reach of the LHC.

### D. Model class II

Figure 8 shows examples of the invariants for class-II models for those cases of sets, which cannot be covered in class I. Again,  $QU$  and  $DL$  are scaled and different plots show differently scaled axes.

The example for set 3 shown in Fig. 8 is similar to the one of the original prototype model constructed in Ref. [20]. For set 6 we have found only a few examples; all of them show invariants which hardly change with respect to the mSugra values of the invariants. The example for set 7 shows that also  $QE$  can decrease considerably in some variants with respect to its mSugra value. Set 8 is quantitatively similar to set 2 and set 16 is quite similar numerically to set 14. To distinguish these, highly accurate SUSY mass measurements would be necessary.

Again we note that larger values of  $\Delta b_3^{LR}$ , especially large  $\Delta b_3^{LR}$ , usually lead to numerically larger changes in the invariants, making these models in principle easier to test.

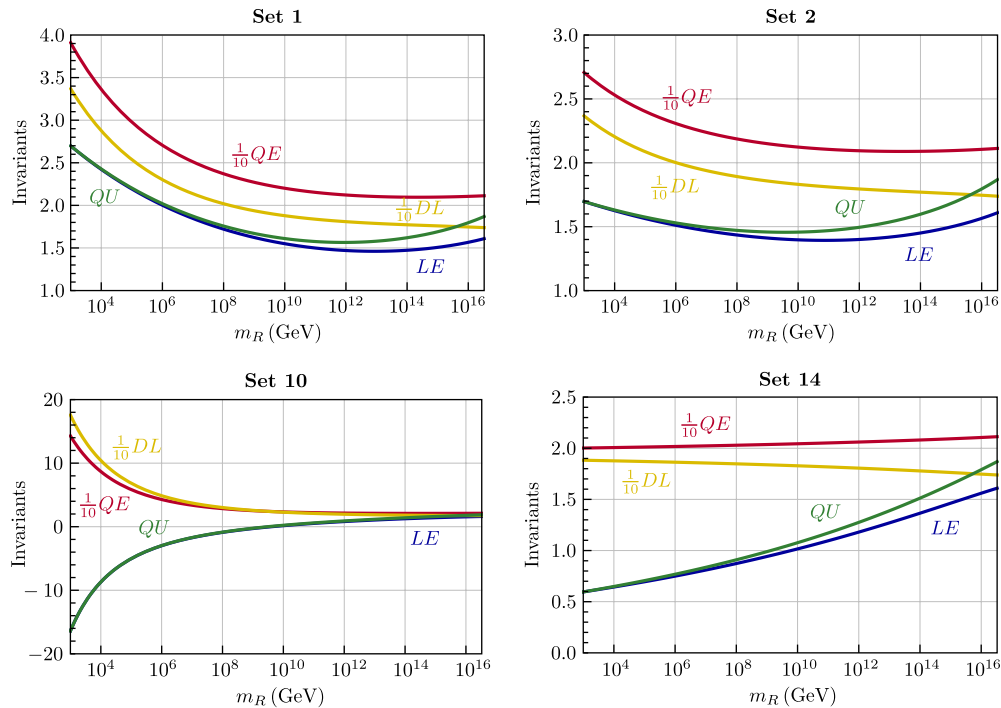


FIG. 7 (color online).  $m_R$  dependence of the invariants in model class I. The examples of  $\Delta b_i^{LR} = (\Delta b_3^{LR}, b_L^{LR}, \Delta b_R^{LR}, \Delta b_{BL}^{LR})$  for these sets are as follows. Set 1: (2, 2, 9, 1/2). Set 2: (1, 1, 7, 1). Set 10: (4, 4, 3, 29/2). Set 14: (0, 0, 2, 6). For a discussion see text.

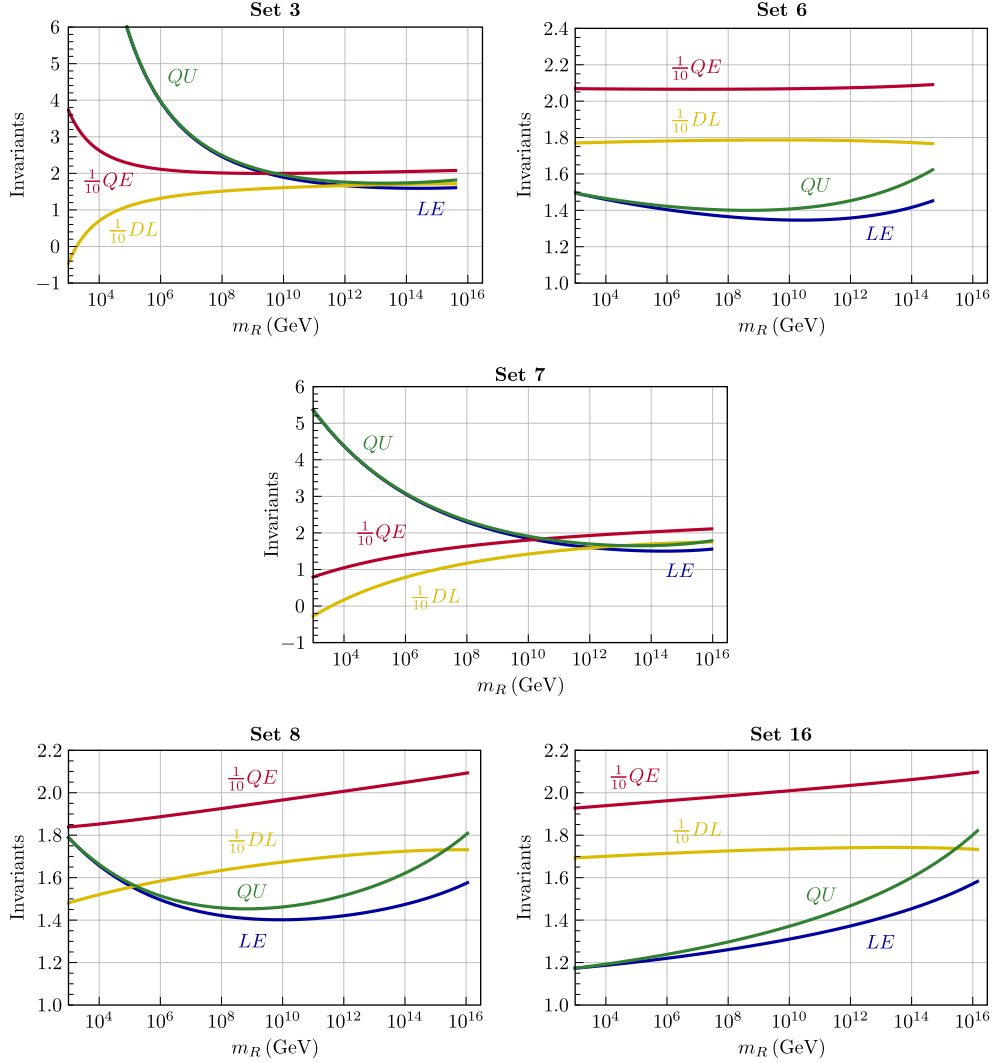


FIG. 8 (color online). The  $m_R$  dependence of the invariants in model class II. The examples shown correspond to the choices of  $\Delta b = (\Delta b_3^{\text{LR}}, \Delta b_L^{\text{LR}}, \Delta b_R^{\text{LR}}, \Delta b_{\text{BL}}^{\text{LR}}, \Delta b_4^{\text{PS}}, \Delta b_L^{\text{PS}}, \Delta b_R^{\text{PS}})$ . Set 3: (0, 1, 10, 3/2, 14, 9, 13). Set 6: (0, 0, 1, 9/2, 63, 60, 114). Set 7: (0, 3, 12, 3/2, 6, 3, 15). Set 8: (0, 0, 9, 3/2, 11, 8, 12). Set 16: (0, 0, 7, 3/2, 11, 8, 10).

### E. Model class III

Here, the invariants depend on  $m_{B-L}$  with a milder or stronger dependence, depending on the value of  $\Delta b_3$ . For almost all the solutions with  $\Delta b_3 = 0$ , the values  $QU$ ,  $DL$ ,  $QE$  are constants and only in  $LE$  a mild variation with  $m_{B-L}$  is found. This fact was already pointed out in Ref. [20]. However, we have found that class-III models can be made with  $\Delta b_3 > 0$  and these, in general, lead to invariants which are qualitatively similar to the case of class I discussed above. In Fig. 9 we show two examples of invariants for class III, one with  $\Delta b_3 = 0$  and one with  $\Delta b_3 = 2$ .

The solutions with  $\Delta b_3 \neq 0$  fall in two kinds: First, the minimum value of  $m_R$  is very large. Then, the invariants have the same behavior than those in which  $\Delta b_3 = 0$ . And, second, the minimum value of  $m_R$  is low. The invariants are not constants and look similar to the ones in the class-I

models. The generally mild dependence on  $m_{B-L}$  can be understood, since it enters into the soft masses only through the changes in the Abelian gauge couplings. Class-III models are therefore the hardest to “test” using invariants.

### F. Comparison of model classes

The classification of variants that we have discussed in Sec. III B only takes into account what happens when the lowest intermediate scale is very low,  $\mathcal{O}(m_{\text{SUSY}})$ . When one varies continuously the lowest intermediate scale ( $m_R$  in the LR- and PS-class models or  $m_{B-L}$  in the BL-class models), each variant draws a line in the four-dimensional space ( $LE$ ,  $QU$ ,  $DL$ ,  $QE$ ). The dimensionality of such a plot can be lowered if we use the (approximate) relations between the invariants shown above, namely  $QU \approx LE$  and  $QE = DL + 2QU$ . We can then choose two

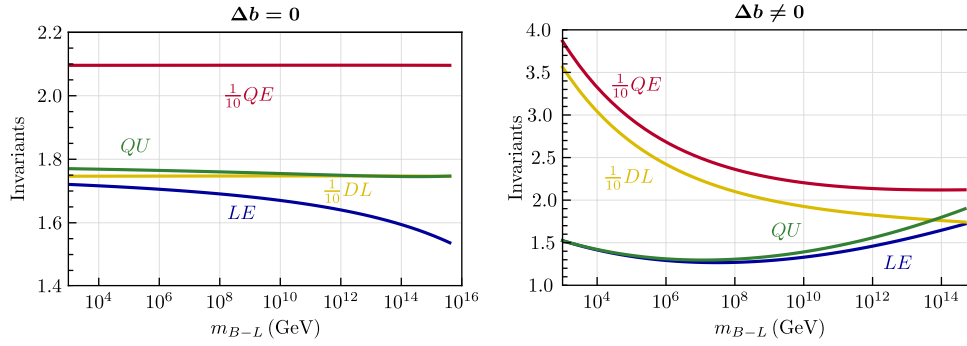


FIG. 9 (color online). The  $m_{B-L}$  dependence of the invariants in class III. To the left the example chooses  $(\Delta b_3^{LR}, \Delta b_L^{LR}, \Delta b_R^{LR}, \Delta b_{BL}^{LR}, \Delta b_3^{BL}, \Delta b_L^{BL}, \Delta \gamma_{RR}, \Delta \gamma_{XR}, \Delta \gamma_{XX}) = (0, 1, 3, 3, 0, 0, 1/2, -\sqrt{3}/8, 3/4)$ . To the right:  $(2, 2, 4, 8, 2, 2, 1/2, -\sqrt{3}/8, 11/4)$ .

independent ones, for example  $LE$  and  $QE$ , so that the only nontrivial information between the four invariants is encoded in a  $(LE, QE)$  plot. In this way, it is possible to simultaneously display the predictions of different variants. This was done in Fig. 10, where LR, PS and BL variants are drawn together. The plot is exhaustive in the sense that it includes all LR variants, as well as all PS and BL variants which can have the highest intermediate scale below  $10^6$  GeV. In all cases, we required that  $\alpha^{-1}$  at unification is larger than  $1/2$  when the lowest intermediate scale is equal to  $m_{\text{SUSY}}$ .

There is a dot in the middle of the figure—the mSugra point—which corresponds to the prediction of mSugra models, in the approximation used. It is expected that every model will draw a line with one end close to this point. This end point corresponds to the limit where the intermediate scales are close to the GUT scale and therefore the running in the LR, PS and BL phases is small so the invariants should be similar to those in mSugra models. So the

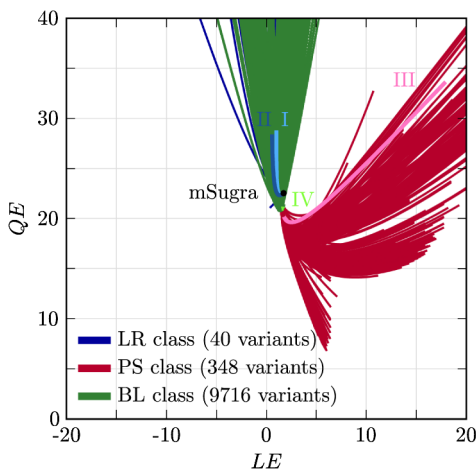


FIG. 10 (color online). Parametric  $(LE, QE)$  plot for the different variants (see text). The thicker lines labeled with I, II, III and IV indicate the results for the four prototype models presented in Ref. [20].

general picture is that lines tend to start (when the lowest intermediate scale is of the order of  $10^3$  GeV) outside or at the periphery of the plot, away from the mSugra point and, as the intermediate scales increase, they converge towards the region of the mSugra point, in the middle of the plot. In fact, note that all the lines of LR-class models do touch this point, because we can slide the LR scale all the way to  $m_G$ . But in PS and BL models there are two intermediate scales and often the lowest one cannot be increased all the way up to  $m_G$ , either because that would make the highest intermediate scale bigger than  $m_G$  or because it would invert the natural ordering of the two intermediate scales.

It is interesting to note that the BL class with low  $m_R$  can produce the same imprint in the sparticle masses as LR models. This is to be expected because with  $m_R$  close to  $m_{B-L}$  the running in the  $U(1)$ -mixing phase is small, leading to predictions similar to LR models. The equivalent limit for PS-class models is reached for very high  $m_{\text{PS}}$ , close to the GUT scale (see below). On the other hand, from Fig. 10 we can see that a low  $m_{\text{PS}}$  actually leads to a very different signal on the soft sparticle masses. For example, a measurement of  $LE \approx 10$  and  $QE \approx 15$ , together with compatible values for the other two invariants ( $QU \approx 10$  and  $DL \approx -5$ ) would immediately exclude *all classes of models except PS models*, and in addition it would strongly suggest low PS and LR scales.

Figure 11 illustrates the general behavior of PS models as we increase the separation between the  $m_{LR}$  and  $m_{\text{PS}}$  scales. The filled region in the  $(LE, QE)$  plot tends to rotate anticlockwise until it reaches, for very high  $m_{\text{PS}}$ , the same region of points which is predicted by LR models. Curiously, we also see in Fig. 11 that some of these models actually predict different invariant values from the ones of LR models. What happens in these cases is that since the PS phase is very short, it is possible to have many active fields in it which decouple at lower energies. So even though the running is short, the values of the different gauge couplings actually get very large corrections in

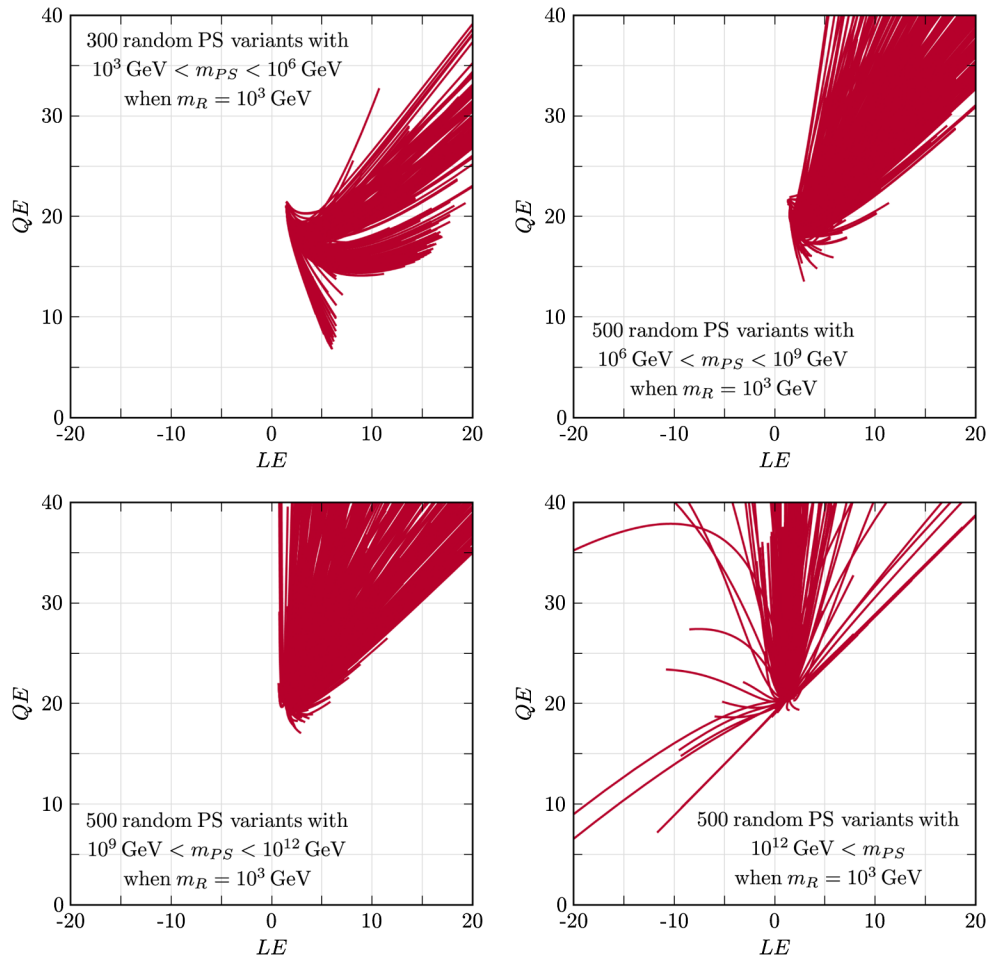


FIG. 11 (color online). Parametric  $(LE, QE)$  plots for different PS variants showing the effect of the PS scale.

this regime and these are uncommon in other settings. For example, it is possible in this special subclass of PS models for  $\alpha_R$  to get bigger than  $\alpha_3/\alpha_4$  before unifying.

One can see from Fig. 11 that many, although not all PS models, can lead to large values of  $LE$ . This can happen for both low and high values of  $m_{PS}$  and is a rather particular feature of the class II, which cannot be found in the other classes.

#### IV. SUMMARY AND CONCLUSIONS

We have discussed  $SO(10)$ -inspired supersymmetric models with extended gauge group near the electroweak scale, consistent with gauge coupling unification thanks to a sliding scale mechanism. We have discussed three different setups, which we call classes of models. The first and simplest chain we use breaks  $SO(10)$  through a left-right symmetric stage to the SM group, and class II uses an additional intermediate Pati-Salam stage, while in class III we discuss models which break the LR-symmetric group first into a  $U(1)_R \times U(1)_{B-L}$  group before reaching the SM group. We have shown that in each case many different

variants and many configurations (or protomodels) for each variant can be constructed.

We have discussed that one cannot only construct sliding models in which an inverse or linear seesaw is consistent with GCU, as done in earlier work [20,22,23], but also all other known types of seesaws can, in principle, be found. We found example configurations for seesaw type I, type II and type III and even inverse type III (for which one example limited to class II was previously discussed in Ref. [20]).

Due to the sliding scale property the different configurations predict potentially rich phenomenology at the LHC, although by the same reasoning the discovery of any of the additional particles the models predict is of course not guaranteed. However, even if all the new particles—including the gauge bosons of the extended gauge group—lie outside of the reach of the LHC, indirect tests of the models are possible from measurements of SUSY particle masses. We have discussed certain combinations of soft parameters, called invariants, and shown that the invariants themselves can be classified into a few sets. Just determining to which set the experimental data belong



would allow us to distinguish, at least in some cases, class-I from class-II models and also in all but one case our classes of models are different from the ordinary high-scale seesaw (type-II and type-III) models. Depending on the accuracy with which supersymmetric masses can be measured in the future, the invariants could be used to gain indirect information not only on the class of model and its variant realized in nature, but also give hints on the scale of beyond-MSSM physics, i.e., the energy scale at which the extended gauge group is broken.

We add a few words of caution. First of all, our analysis is done completely at the 1-loop level. It is known from numerical calculations for seesaw type II [26] and seesaw type III [27] that the invariants receive numerically important shifts at 2-loop level. In addition, there are also uncertainties in the calculation from GUT-scale thresholds and from uncertainties in the input parameters. For the latter the most important is most likely the error on  $\alpha_S$  [20]. With the huge number of models we have considered, taking into account all of these effects is impractical and, thus, our numerical results should be taken as approximate. However, should any signs of supersymmetry be found in the future, improvements in the calculations along these lines could be easily made, should it become necessary. More important for the calculation of the invariants is, of course, the assumption that SUSY breaking indeed is mSugra-like. Tests of the validity of this assumption can be made also only indirectly. Many of the spectra we find, especially in the class-II models, are actually quite different from standard mSugra expectations and thus a pure MSSM-mSugra would give a bad fit to experimental data, if one of these models is realized in nature. However, all of our variants still fulfill (by construction) a certain sum rule; see the discussion in Sec. III B.

Of course, so far no signs of supersymmetry have been seen at the LHC, but with the planned increase of  $\sqrt{s}$  for the next run of the accelerator there is still quite a lot of parameter space to be explored. We note in this respect that we are not overly concerned about the Higgs mass,  $m_h \sim (125\text{--}126)$  GeV, if the new resonance found by the ATLAS [42] and CMS [43] collaborations turns out to be indeed the lightest Higgs boson. While for a pure MSSM with mSugra boundary conditions it is well known [44–47] that such a hefty Higgs requires multi-TeV scalars,<sup>9</sup> all our models have an extended gauge symmetry. Thus, there are new D-terms contributing to the Higgs mass [49,50], alleviating the need for large soft SUSY breaking terms, as has been explicitly shown in Refs. [51,52] for one particular realization of a class-III model [20,22].

Finally, many of the configurations (or protomodels) which we have discussed contain exotic superfields, which

might show up in the LHC. It might therefore be interesting to do a more detailed study of the phenomenology of at least some particular examples of the models we have constructed.

## ACKNOWLEDGMENTS

This work has been supported in part by EU Network Grant No. UNILHC PITN-GA-2009-237920. M.H. also acknowledges support from the Spanish MICINN Grants No. FPA2011-22975, No. MULTIDARK CSD2009-00064 and by the Generalitat Valenciana Grant No. Prometeo/2009/091. The work of R.M.F. has been supported by *Fundação para a Ciência e a Tecnologia* through the fellowship SFRH/BD/47795/2008. R.M.F. and J.C.R. also acknowledge the financial support from Grants No. CFTP-FCT UNIT 777, No. CERN/FP/123580/2011 and No. PTDC/FIS/102120/2008.

## APPENDIX: LISTS OF SUPERFIELDS

We have considered  $SO(10)$ -inspired models which may contain any irreducible representation up to dimension 126 (**1**, **10**, **16**,  $\overline{\mathbf{16}}$ , **45**, **54**, **120**, **126**,  $\overline{\mathbf{126}}$ ). Once the gauge group breaks down to  $SU(4) \times SU(2)_L \times SU(2)_R$  or  $SU(3)_C \times SU(2)_L \times SU(2)_R \times U(1)_{B-L}$  these  $SO(10)$  fields divide into a multitude of different irreducible representation of these groups. In addition, if  $SU(2)_R$  is broken down further to  $U(1)_R$  the following branching rules apply:  $\mathbf{3} \rightarrow -1, 0, +1$ ;  $\mathbf{2} \rightarrow \pm \frac{1}{2}$ ;  $\mathbf{1} \rightarrow 0$ . The standard model's hypercharge, in the canonical normalization, is then equal to the combination  $\sqrt{\frac{3}{5}}[U(1)_R \text{ hypercharge}] + \sqrt{\frac{2}{5}}[U(1)_{B-L} \text{ hypercharge}]$ . In Tables IV, V, and VI we present the list of relevant fields respecting the conditions above. In these tables we used an ordered naming of the fields. Sometimes it is also useful, like in Table I, to indicate explicitly the quantum numbers under the various groups.

In order for a group  $G$  to break into a subgroup  $H \subset G$ , there must be a field transforming nontrivially under  $G$  which contains a singlet of  $H$  that acquires vacuum expectation value. From this observation alone we know that certain fields must be present in a fundamental model if we are to achieve a given breaking sequence:

- (i) The breaking  $PS \rightarrow LR$  is possible only with the (**15**, **1**, **1**) while  $PS \rightarrow 3211$  requires the combination (**15**, **1**, **1**) + (**1**, **1**, **3**). For the direct breaking  $PS \rightarrow 321$  there are two choices: (**4**, **1**, **2**), (**10**, **1**, **3**) or their conjugates;
- (ii) The breaking  $LR \rightarrow 3211$  requires the (**1**, **1**, **3**, **0**) representation while the direct route  $LR \rightarrow 321$  is possible with the presence of (**1**, **1**, **2**,  $-1$ ), (**1**, **1**, **3**,  $-2$ ) or their conjugates;
- (iii) The group 3211 can be broken down to 321 with the representations (**1**, **1**,  $\frac{1}{2}$ ,  $-1$ ), (**1**, **1**, **1**,  $-2$ ) or their conjugates.

<sup>9</sup>Multi-TeV scalars are also required, if the MSSM with mSugra boundary conditions is extended to include a high-scale seesaw mechanism [48].

TABLE IV. Naming conventions and transformation properties of fields in the left-right symmetric regime (not considering conjugates). The charges under the  $U(1)_{B-L}$  group shown here were multiplied by a factor  $\sqrt{\frac{8}{3}}$ .

	$\Phi_1$	$\Phi_2$	$\Phi_3$	$\Phi_4$	$\Phi_5$	$\Phi_6$	$\Phi_7$	$\Phi_8$	$\Phi_9$	$\Phi_{10}$	$\Phi_{11}$	$\Phi_{12}$	$\Phi_{13}$	$\Phi_{14}$	$\Phi_{15}$	$\Phi_{16}$	$\Phi_{17}$	$\Phi_{18}$	$\Phi_{19}$	$\Phi_{20}$	$\Phi_{21}$	$\Phi_{22}$	$\Phi_{23}$	$\Phi_{24}$
	$\chi$	$\chi^c$	$\Omega$	$\Omega^c$	$\Phi$			$\delta_d$	$\delta_u$							$\Delta$	$\Delta^c$							
$SU(3)_C$	1	1	1	1	1	1	8	1	3	3	6	6	3	3	8	1	1	3	3	3	6	6	1	3
$SU(2)_L$	1	2	1	3	1	2	1	1	1	1	1	1	2	1	2	3	1	2	3	1	3	1	3	2
$SU(2)_R$	1	1	2	1	3	2	1	1	1	1	1	1	2	2	1	3	2	1	3	1	3	3	3	2
$U(1)_{B-L}$	0	+1	-1	0	0	0	0	+2	$-\frac{2}{3}$	$+\frac{4}{3}$	$+\frac{2}{3}$	$-\frac{4}{3}$	$+\frac{1}{3}$	$+\frac{1}{3}$	0	-2	-2	$+\frac{4}{3}$	$-\frac{2}{3}$	$-\frac{2}{3}$	$+\frac{2}{3}$	$+\frac{2}{3}$	0	$-\frac{2}{3}$
PS	$\Psi_1$					$\Psi_2$	$\Psi_{10}$		$\Psi_8$										$\Psi_{14}$	$\Psi_{15}$				
Origin	$\Psi_{10}$	$\bar{\Psi}_{12}$	$\Psi_{13}$	$\Psi_3$	$\Psi_4$	$\Psi_7$	$\Psi_{11}$	$\bar{\Psi}_9$	$\Psi_{10}$	$\Psi_9$	$\Psi_{11}$	$\Psi_{12}$	$\Psi_{13}$	$\Psi_7$	$\Psi_{16}$	$\Psi_{17}$	$\Psi_7$		$\Psi_{16}$	$\Psi_{17}$	$\Psi_5$	$\Psi_6$		

TABLE V. Naming conventions and transformation properties of fields in the Pati-Salam regime (not considering conjugates).

	$\Psi_1$	$\Psi_2$	$\Psi_3$	$\Psi_4$	$\Psi_5$	$\Psi_6$	$\Psi_7$	$\Psi_8$	$\Psi_9$	$\Psi_{10}$	$\Psi_{11}$	$\Psi_{12}$	$\Psi_{13}$	$\Psi_{14}$	$\Psi_{15}$	$\Psi_{16}$	$\Psi_{17}$
$SU(4)$	1	1	1	1	1	6	15	6	10	15	20'	4	4	6	6	10	10
$SU(2)_L$	1	2	3	1	3	2	2	1	1	1	1	2	1	3	1	3	1
$SU(2)_R$	1	2	1	3	3	2	2	1	1	1	1	2	1	3	1	3	1
$SO(10)$	1	10				45	120	10									
Origin	54	120	45	45	54	54	126	126	120	45	54	16	$\bar{16}$	120	120	126	$\bar{126}$

TABLE VI. Naming conventions and transformation properties of fields in the  $U(1)$  mixing regime (not considering conjugates). The charges under the  $U(1)_{B-L}$  group shown here were multiplied by a factor  $\sqrt{\frac{8}{3}}$ .

	$\Phi'_1$	$\Phi'_2$	$\Phi'_3$	$\Phi'_4$	$\Phi'_5$	$\Phi'_6$	$\Phi'_7$	$\Phi'_8$	$\Phi'_9$	$\Phi'_{10}$	$\Phi'_{11}$	$\Phi'_{12}$	$\Phi'_{13}$	$\Phi'_{14}$	$\Phi'_{15}$	$\Phi'_{16}$	$\Phi'_{17}$	$\Phi'_{18}$	$\Phi'_{19}$	$\Phi'_{20}$	$\Phi'_{21}$	$\Phi'_{22}$	$\Phi'_{23}$	$\Phi'_{24}$	$\Phi'_{25}$	$\Phi'_{26}$	$\Phi'_{27}$	$\Phi'_{28}$	$\Phi'_{29}$	$\Phi'_{30}$	$\Phi'_{31}$
$SU(3)_C$	1	1	1	1	1	1	8	1	3	3	6	6	3	3	3	8	1	1	1	3	3	3	3	3	3	6	6	6	1	3	3
$SU(2)_L$	1	2	1	3	1	2	1	1	1	1	1	1	2	1	2	3	1	1	2	2	3	1	1	3	1	1	3	1	3	2	2
$U(1)_R$	0	0	$-\frac{1}{2}$	$+\frac{1}{2}$	0	+1	$+\frac{1}{2}$	0	0	0	0	0	0	0	$-\frac{1}{2}$	$+\frac{1}{2}$	$+\frac{1}{2}$	0	-1	+1	$-\frac{1}{2}$	$+\frac{1}{2}$	0	-1	+1	0	-1	+1	+1	$-\frac{1}{2}$	$+\frac{1}{2}$
$U(1)_{B-L}$	0	+1	-1	-1	0	0	0	+2	$-\frac{2}{3}$	$+\frac{4}{3}$	$+\frac{2}{3}$	$-\frac{4}{3}$	$+\frac{1}{3}$	$+\frac{1}{3}$	$+\frac{1}{3}$	0	-2	-2	-2	$+\frac{4}{3}$	$+\frac{4}{3}$	$-\frac{2}{3}$	$-\frac{2}{3}$	$-\frac{2}{3}$	$+\frac{2}{3}$	$+\frac{2}{3}$	$+\frac{2}{3}$	0	$-\frac{2}{3}$	$-\frac{2}{3}$	
LR	$\Phi_1$			$\Phi_4$			$\Phi_8$	$\Phi_9$		$\Phi_{11}$																					
Origin	$\Phi_5$	$\Phi_2$	$\Phi_3$	$\Phi_3$	$\Phi_5$	$\Phi_6$	$\Phi_7$		$\Phi_{10}$	$\Phi_{12}$	$\Phi_{13}$	$\Phi_{14}$	$\Phi_{14}$	$\Phi_{15}$	$\Phi_{16}$	$\Phi_{17}$	$\Phi_{17}$	$\Phi_{18}$	$\Phi_{18}$	$\Phi_{19}$	$\Phi_{20}$	$\Phi_{20}$	$\Phi_{21}$	$\Phi_{22}$	$\Phi_{22}$	$\Phi_{22}$	$\Phi_{23}$	$\Phi_{24}$	$\Phi_{24}$		

- [1] Y. Fukuda *et al.* (Super-Kamiokande Collaboration), *Phys. Rev. Lett.* **81**, 1562 (1998).
- [2] Q. Ahmad *et al.* (SNO Collaboration), *Phys. Rev. Lett.* **89**, 011301 (2002).
- [3] K. Eguchi *et al.* (KamLAND Collaboration), *Phys. Rev. Lett.* **90**, 021802 (2003).
- [4] D. Forero, M. Tortola, and J. W. F. Valle, *Phys. Rev. D* **86**, 073012 (2012).
- [5] P. Minkowski, *Phys. Lett.* **67B**, 421 (1977).
- [6] T. Yanagida, in *KEK Lectures*, edited by O. Sawada and A. Sugamoto (World Scientific, Tsukuba, Japan, 1979).
- [7] M. Gell-Mann, in *Supergravity*, edited by P. Van Nieuwenhuizen and D.Z. Freedman (North-Holland, Amsterdam, 1979).
- [8] R.N. Mohapatra and G. Senjanovic, *Phys. Rev. Lett.* **44**, 912 (1980).
- [9] H. Fritzsch and P. Minkowski, *Ann. Phys.* **93**, 193 (1975).
- [10] R.N. Mohapatra, *Contemporary Physics* (Springer, Berlin, 1986).
- [11] C.S. Aulakh and R.N. Mohapatra, *Phys. Rev. D* **28**, 217 (1983).
- [12] T.E. Clark, T.-K. Kuo, and N. Nakagawa, *Phys. Lett.* **115B**, 26 (1982).
- [13] C.S. Aulakh, B. Bajc, A. Melfo, A. Rasin, and G. Senjanovic, *Nucl. Phys.* **B597**, 89 (2001).
- [14] C.S. Aulakh, B. Bajc, A. Melfo, G. Senjanovic, and F. Vissani, *Phys. Lett. B* **588**, 196 (2004).
- [15] M. Cvetič and J.C. Pati, *Phys. Lett.* **135B**, 57 (1984).

- [16] R. Kuchimanchi and R. Mohapatra, *Phys. Rev. D* **48**, 4352 (1993).
- [17] C. S. Aulakh, K. Benakli, and G. Senjanovic, *Phys. Rev. Lett.* **79**, 2188 (1997).
- [18] C. S. Aulakh, A. Melfo, A. Rasin, and G. Senjanovic, *Phys. Rev. D* **58**, 115007 (1998).
- [19] S. K. Majee, M. K. Parida, A. Raychaudhuri, and U. Sarkar, *Phys. Rev. D* **75**, 075003 (2007).
- [20] V. De Romeri, M. Hirsch, and M. Malinsky, *Phys. Rev. D* **84**, 053012 (2011).
- [21] L. Calibbi, L. Ferretti, A. Romanino, and R. Ziegler, *Phys. Lett. B* **672**, 152 (2009).
- [22] M. Malinsky, J. Romao, and J. W. F. Valle, *Phys. Rev. Lett.* **95**, 161801 (2005).
- [23] P. B. Dev and R. Mohapatra, *Phys. Rev. D* **81**, 013001 (2010).
- [24] J. C. Pati and A. Salam, *Phys. Rev. D* **10**, 275 (1974).
- [25] M. R. Buckley and H. Murayama, *Phys. Rev. Lett.* **97**, 231801 (2006).
- [26] M. Hirsch, S. Kaneko, and W. Porod, *Phys. Rev. D* **78**, 093004 (2008).
- [27] J. Esteves, J. Romao, M. Hirsch, F. Staub, and W. Porod, *Phys. Rev. D* **83**, 013003 (2011).
- [28] K. S. Babu and R. N. Mohapatra, *Phys. Rev. Lett.* **70**, 2845 (1993).
- [29] B. Bajc, G. Senjanovic, and F. Vissani, *Phys. Rev. Lett.* **90**, 051802 (2003).
- [30] J. Beringer *et al.* (Particle Data Group), *Phys. Rev. D* **86**, 010001 (2012).
- [31] J. Romao *et al.*, <http://porthos.ist.utl.pt/arXiv/AllSO10GUTs>.
- [32] R. N. Mohapatra and J. W. F. Valle, *Phys. Rev. D* **34**, 1642 (1986).
- [33] E. K. Akhmedov, M. Lindner, E. Schnapka, and J. W. F. Valle, *Phys. Lett. B* **368**, 270 (1996).
- [34] E. K. Akhmedov, M. Lindner, E. Schnapka, and J. W. F. Valle, *Phys. Rev. D* **53**, 2752 (1996).
- [35] R. Foot, H. Lew, X. He, and G. C. Joshi, *Z. Phys. C* **44**, 441 (1989).
- [36] K. Babu, B. Dutta, and R. Mohapatra, *Phys. Rev. D* **60**, 095004 (1999).
- [37] S. Davidson, D. C. Bailey, and B. A. Campbell, *Z. Phys. C* **61**, 613 (1994).
- [38] A. Kuznetsov, N. Mikheev, and A. Serghienko, [arXiv:1210.3697](https://arxiv.org/abs/1210.3697).
- [39] R. M. Fonseca, M. Malinsky, W. Porod, and F. Staub, *Nucl. Phys.* **B854**, 28 (2012).
- [40] H. Baer, V. Barger, A. Lessa, and X. Tata, *Phys. Rev. D* **86**, 117701 (2012).
- [41] G. Aad *et al.* (ATLAS Collaboration), Report No. ATLAS-CONF-2012-109, 2012.
- [42] G. Aad *et al.* (ATLAS Collaboration), *Phys. Lett. B* **716**, 1 (2012).
- [43] S. Chatrchyan *et al.* (CMS Collaboration), *Phys. Lett. B* **716**, 30 (2012).
- [44] A. Arbey, M. Battaglia, A. Djouadi, F. Mahmoudi, and J. Quevillon, *Phys. Lett. B* **708**, 162 (2012).
- [45] H. Baer, V. Barger, and A. Mustafayev, *Phys. Rev. D* **85**, 075010 (2012).
- [46] O. Buchmueller *et al.*, *Eur. Phys. J. C* **72**, 2020 (2012).
- [47] J. Ellis and K. A. Olive, *Eur. Phys. J. C* **72**, 2005 (2012).
- [48] M. Hirsch, F. Joaquim, and A. Vicente, *J. High Energy Phys.* **11** (2012) 105.
- [49] H. E. Haber and M. Sher, *Phys. Rev. D* **35**, 2206 (1987).
- [50] M. Drees, *Phys. Rev. D* **35**, 2910 (1987).
- [51] M. Hirsch, W. Porod, L. Reichert, and F. Staub, *Phys. Rev. D* **86**, 093018 (2012).
- [52] M. Hirsch, M. Malinsky, W. Porod, L. Reichert, and F. Staub, *J. High Energy Phys.* **02** (2012) 084.